# Chain architecture as an orthogonal parameter to influence block copolymer morphology. The synthesis and characterisation of hyperbranched block copolymers - HyperBlocks.

*Lian. R. Hutchings*[1], Serena Agostini, Ian Hamley[2] and Daniel Hermida-Merino[3]*

[1]Durham Centre for Soft Matter, Department of Chemistry, Durham University, Durham DH1 3LE, United Kingdom.

[2]Department of Chemistry, University of Reading, Whiteknights, Reading, RG6 6AD, United Kingdom.

[3]ESRF - The European Synchrotron, CS 40220, 38043 Grenoble, Cedex 9, France

KEYWORDS HyperBlocks, thermoplastic elastomers, living anionic polymerisation, macromonomers.

ABSTRACT. For block copolymers there is usually a strong correlation between the copolymer composition (volume fraction of each block) and the resulting solid state morphology. However, for a variety of potential applications, e.g., semipermeable membranes or templates, it might be desirable to vary the microphase morphology independently of copolymer composition. The use of chain branching is an additional and

orthogonal parameter to influence morphology, independently of composition and we explore for the first time, the impact of a long-chain, hyperbranched architecture on the microphase separated, solid-state morphology of branched block copolymers. To this end a series of functionalised linear ABA (polystyrene-polyisoprene-polystyrene) triblock copolymers (macromonomers), hyperbranched ABA triblock copolymers (HyperBlocks) and blends of HyperBlocks with a commercially available linear ABA triblock copolymeric thermoplastic elastomer were prepared. Moreover, the "macromonomer" approach is the only feasible route to prepare hyperbranched block copolymers. The solid-state morphology of the resulting materials was investigated by a combination of transmission electron microscopy (TEM) and small-angle X-ray scattering (SAXS) which showed a dramatic impact of the chain architecture on the resulting morphology. Whilst the linear ABA triblock copolymers showed the expected microphase-separated morphology with long-range order dependent upon composition, no long-range order was observed in the HyperBlocks. Instead the HyperBlocks revealed a microphase-separated morphology without long-range lattice order, irrespective of macromonomer composition or molecular weight. Furthermore, when HyperBlocks were subsequently blended with a commercially available linear ABA triblock copolymer (Kraton D1160$^{TM}$) the HyperBlock appeared to *impose* a microphase separated morphology *without* long-range lattice order upon the linear copolymer even when the HyperBlock is present as the minor component in the blend at levels as low as 10% by weight.

**Introduction**

It is well known that branched polymers possess properties which are fundamentally different from their linear counterparts. Numerous studies on the synthesis and characterisation of model branched polymers have been carried out in order to gain an understanding of the relationship between structure and properties. Predominantly these studies have been aimed at understanding the impact of chain branching upon the melt

rheology of such polymers. Commonly studied branched architectures include the simplest branched structure, star polymers [1-5], and increasingly complex architectures such as mikto-arm stars [6,7], graft/comb polymers [8-13], H-shaped polymers [14-17] and dendritically long-chain branched polymers [18-28]. Chain-branching in block copolymers has also been explored with a view to understand the influence of architecture upon phase separation. In one of the earliest studies[29] Price *et al* in 1972 prepared a series of diblock, triblock, and three- and four-arm star block copolymers of isoprene and styrene with constant volume of the styrene. Electron microscopy on solvent-cast films revealed hexagonally packed cylinders of polystyrene in a polyisoprene matrix for all arm numbers. It was reported that arm number had no effect on domain diameter or spacing for two molecular weights. This work was extended by Thomas *et al* [30] who studied the effect of arm number, $f$, ($f$ = 2-18) and arm molecular weight on the solid-state morphology of poly(styrene-isoprene) star-block copolymers. It was reported that the morphology varied as a function of arm number and when $f$ >8, an ordered bicontinuous morphology was observed when a linear block copolymer of equivalent composition forms polystyrene cylinders, hexagonally packed in the polydiene matrix. More than two decades ago Milner[31] discussed the impact of branching in mikto arm stars with $n$ (where $n$ = 2 or 3) arms of polymer A and one arm of B. He made predictions, supported by experimental data[32,33] that the architecture would influence interfacial curvature and morphology such that for a fixed volume fraction $\Phi_B$ = 0.4 (assuming elastically symmetric blocks), a diblock copolymer ($n_A = n_B = 1$) would form lamellae, a three arm star ($n_A = 2$) would form cylinders and a four arm star ($n_A = 3$) would form spheres. Much of the extensive early work on star-branched copolymers and more complex branched block copolymers is summarised in a couple of nice reviews[34,35] on the subject . More recently Mays *et al* [36-38] have studied the impact of architecture on solid state morphology for a series of graft copolymers comprising of polyisoprene backbones with polystyrene grafts. The grafts were arranged with regularly

spaced branch points of varying functionality (tri-, tetra- and hexafunctional) and whilst observed morphologies were in line with expectations based on theoretical predictions[31], long range order decreased dramatically as the number of branch points increased for constant volume fraction of polystyrene.

One interesting sub-class of dendritically long-chain branched polymers is long-chain hyperbranched polymers (LCHBPs) which are characterised by a high degree of branching, and various degrees of irregularity in branching structure and molecular weight between branch points. These highly-branched polymers are generally prepared in a facile, one-pot synthesis and the synthetic methodologies result in randomly branched polymers with broad molecular weight distributions. Various approaches have been reported for the synthesis of such polymers and this topic has been the subject of a recent review[39]. Common approaches to introduce a linear polymer segment between branching points in LCHBPs include self-condensing vinyl polymerisation (SCVP)[40-43] and the so called "Strathclyde approach"[44] which exploits radical polymerisation, a divinyl comonomer and a chain transfer agent to prevent gelation. Knauss[45-47] reported the synthesis of dendritically branched polystyrene prepared by anionic polymerization in which styrene was polymerized in the presence of either vinylbenzyl chloride (VBC) or 4-(chlorodimethylsilyl)styrene (CDMSS). Each comonomer is capable of a dual role; the vinyl group enables VBC and CDMSS to take part in the polymerization and the chloromethyl/chlorosilane functionalities are susceptible to nucleophilic attack by polystyryllithium resulting in the introduction of a branching point.

However, the methods described above offer little or no control over the molecular weight of the linear segment between branch points. Only the 'macromonomer' approach, widely reported by ourselves[48-51], which uses functionalized linear polymeric chains (macromonomers) as building blocks, is capable of producing highly (hyper)branched polymers in which the molecular weight of the linear segments can be controlled. Probably

the first example of the macromonomer approach to prepare hyperbranched polymers was the work of Hedrick *et al*[52,53], who reported the synthesis of $AB_2$ macromonomers of poly(ε-caprolactone) (PCL) and their use in the synthesis of hyperbranched PCL. A similar approach was subsequently reported by us for the synthesis of macromonomers from vinyl monomers for the first time, in the production of polystyrene HyperMacs[48,51]. This involved the synthesis of an α,ω-$AB_2$ polystyrene macromonomer by living anionic polymerization, thereby offering maximum control over molecular weight and dispersity with macromonomer molecular weights up to 100,000 $gmol^{-1}$. The polystyrene macromonomers, decorated with reactive end-group functionalities comprising of two phenols (B) and a halide (chloride[48] or bromide[51]) group (A), undergo a (polycondensation) Williamson coupling reaction to produce the branched HyperMacs. This strategy was subsequently extended to include the synthesis of HyperMacs from poly(methylmethacrylate) and polybutadiene[54] and model asymmetric polystyrene star polymers[55]. Moreover, the macromonomer approach to make LCHB polymers is unique in being able to make hyperbranched block copolymers, HyperBlocks, exemplified in the production of an ABA triblock copolymeric macromonomer of polyisoprene-polystyrene-polyisoprene and first reported by ourselves in a proof of concept study[54]. In recent years the 'macromonomer' approach to make LCHBPs has been widely adopted with reported examples of macromonomers produced by ring opening metathesis polymerization (ROMP)[56-59], reversible-addition chain transfer polymerization (RAFT)[60,61], atom transfer radical polymerization (ATRP)[62-66], anionic polymerization[67,68], ring opening polymerization[69,70] and polycondensation reactions[71]. Various coupling strategies have been used to convert these linear macromonomers into LCBHPs including thiol-yne[60,61] and azide-alkyne[56-58,62-65, 70] click reactions, esterification[59] and hydrosilylation[67] reactions.

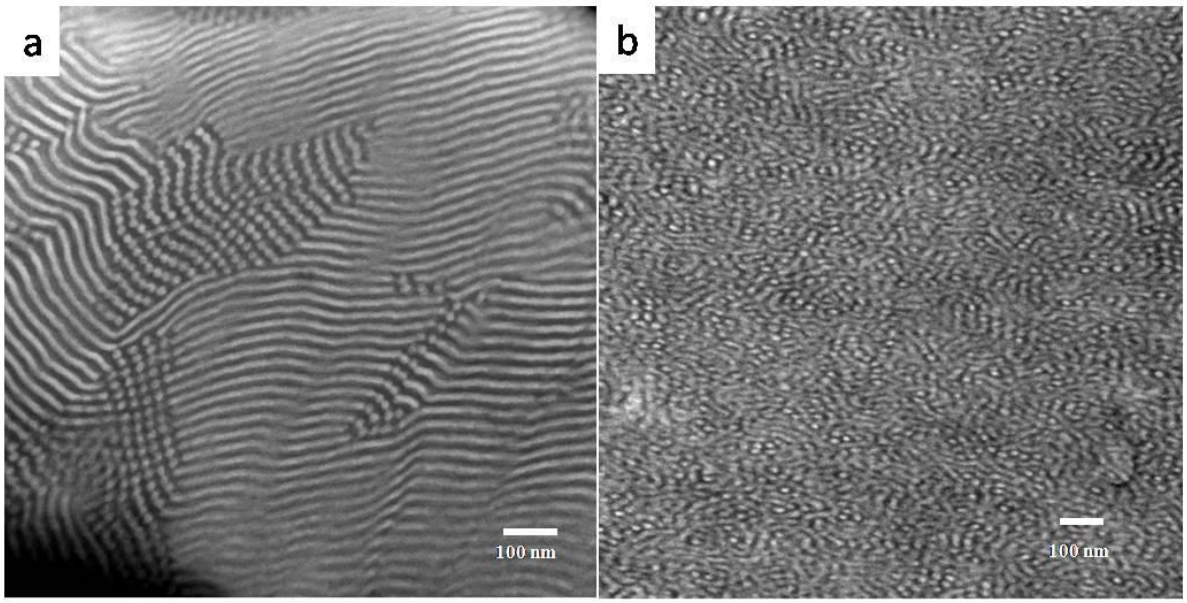


**Figure 1.** TEM micrograms of a) PS-PI-PS linear macromonomer and b) PS-PI-PS HyperBlock[54]

In the proof of principle study in which the concept of HyperBlocks was first reported[54], a single sample of a HyperBlock was synthesised and analysed by TEM and tensile testing to obtain information about the influence of architecture on solid-state morphology and mechanical properties. The macromonomer used in this case was an ABA triblock copolymer of polystyrene and polyisoprene with chain-end functionalities, phenol and bromide, to enable a Williamson coupling reaction for the synthesis of the HyperBlock. The linear macromonomer had a total molar mass of approximately 60 000 g $mol^{-1}$ and a total styrene content of 40% (by mass). The resulting HyperBlock had a molecular weight of about 900,000 $gmol^{-1}$ ($M_w$) and a Đ value of 2.9. Linear block copolymers show a very clear relationship between copolymer composition and morphology and the linear PS-PI-PS macromonomer showed microphase separation with a very well-defined cylindrical morphology, in line with expectations[72], comprising of cylinders of polystyrene within a matrix of polyisoprene and a high degree of long range order (figure 1a). However, the morphology of the HyperBlock derived from this macromonomer was dramatically different.

In figure 1b we can see that the HyperBlock shows microphase separation but with no long range order at all. In terms of composition these two samples are identical; they differ only in terms of molecular weight and molecular architecture. Although it is to be expected that the higher molecular weight HyperBlock might take longer to reach equilibrium morphology we believe that the sample preparation method gives ample time for equilibration and yet we see no long range order. More recently, analogous observations have been made about hyperbranched block copolymers of polystyrene-PCL prepared by a combination of ATRP, ring opening polymerization and "click" coupling reactions[73]. In this case the branched architecture was observed to have a significant impact upon crystallization of the PCL blocks and the authors reported that the degree of crystallinity decreased dramatically when the weight fraction of hyperbranched copolymer in macromonomer/hyperbranched copolymer blend films exceeds ~67%, suggesting that the "uncrystallizable" hyperbranched chains may impose some extra restriction on the crystallization of the linear macromonomer chains. A number of other very recent examples of hyperbranched block copolymers synthesized via a macromonomer approach have also been reported[74,75].

Given the wide commercial exploitation of block copolymers, our initial brief study inspired us to carry out an extended investigation on the properties of HyperBlocks. A series of HyperBlocks has thus been prepared in the current study, with a systematic variation in molecular weight and copolymer composition of the macromonomer in order to understand the interplay between composition and molecular weight of the linear segment, the branched architecture and the resulting physical properties such as solid state morphology. In the present work we report developments in the synthesis of the HyperBlocks and describe the characterisation, by TEM and SAXS, of the macromonomers, HyperBlocks and blends of HyperBlocks with a commercial thermoplastic elastomer, i.e. Kraton$^{TM}$ D1160, a linear polystyrene-polyisoprene-polystyrene triblock copolymer. The effect of the hyperbranched

architecture on the morphology will be described, together with remarkable observations on the changes imposed on the morphology of Kraton$^{TM}$ D1160 when blended with relatively small quantities of HyperBlocks.

## Experimental Section

**Materials.** Benzene (Aldrich, HPLC grade, ≥ 99%), styrene (Sigma-Aldrich, ≥ 99%) and dichloromethane (in-house solvent purification system) were dried and degassed over calcium hydride ($CaH_2$) (Acros Organics, 93%) and stored under high vacuum. 3-*tert*-butyldimethylsiloxy-1-propyllithium in cyclohexane (InitiaLi 103, FMC Corporation), triphenylphosphine, carbon tetrabromide (99%), cesium carbonate, sodium azide (≥ 99.5%) copper sulphate pentahydrate ($CuSO_4 \cdot 5H_2O$), (+)-sodium L-ascorbate, 1,1,1,-tris(4-hydroxyphenyl)ethane (98+%) and N,N,N'N'-tetramethylethylenediamine (all Sigma-Aldrich) were used as received. Dimethyl formamide (DMF) (Sigma-Aldrich 99.8%) was stored over molecular sieves (Sigma-Aldrich) under inert atmosphere. *Sec*-butyllithium (Sigma-Aldrich) 1.4M solution in cyclohexane, and di-*n*-butylmagnesium (Sigma-Aldrich 1.0M solution in heptane were used as received. Propargyl bromide (Sigma-Aldrich) 80 wt. % solution in toluene was used as received. Tetrahydrofuran, methanol (AR grade) and hydrochloric acid (~36 wt. %) (all Fischer Scientific) were used as received. 1,1-Bis(4-*tert*-butyldimethylsiloxyphenyl)ethylene (DPE) was synthesised in two steps from dihydroxybenzophenone according to the procedure of Quirk and Wang.[76]

**Measurements.** $^1$H-NMR spectra were measured on Varian VNMRS 700 MHz or Bruker DRX-400 MHz spectrometer using $C_6D_6$, $D_6$MSO or $CDCl_3$ as solvents.

Triple detection size exclusion chromatography (SEC) was used for the analysis of molecular weight and molecular weight distribution of the macromonomers and Hyperblock polymers, using a Viscotek TDA 302 with refractive index, right angle light scattering and viscosity detectors and two PLgel 5 μm mixed C columns (300 x 75 mm). Tetrahydrofuran

was used as the eluent at a flow rate of 1.0 ml/min and at a temperature of 35 °C. The calibration was carried out with a single narrow distribution polystyrene standard purchased from Polymer Laboratories. A value of 0.185 mL/g (obtained from Viscotek) was used as the dn/dc of polystyrene both for the calibration and the analysis of prepared polymers.

The preparation of the polymers films submitted for transmission electron microscopy (TEM) analysis was carried out by solvent casting. Macromonomers, pure HyperBlocks and blends of 10 and 30 wt. % of HyperBlocks with Kraton$^{TM}$ D-1160 were cast from solutions (6% w/v for HyperBlocks and 30% for macromonomers) in toluene onto aluminium plates. The films were allowed to dry at room temperature and atmospheric pressure for one day and then under vacuum to constant weight. Samples for TEM analysis were prepared by cryo-ultramicrotomy using a Leica EM UC6 Ultramicrotome and Leica EM FC6 cryochamber (Milton Keynes, UK). Cryosections of 50–70 nm thickness were cut using a cryo 35° diamond knife (Diatome, Switzerland) at a temperature between -120°C and -140°C and then manipulated from the knife edge onto formvar coated grid. Sections were stained for 2-4 hrs with osmium tetroxide ($OsO_4$) vapour then viewed with a Hitachi H7600 transmission electron microscope (Hitachi High Technologies Europe) using an accelerating voltage of 100KV.

Small angle X-ray scattering (SAXS) measurements were performed on polymer films prepared by solvent casting. A solution in toluene of macromonomers, pure HyperBlocks or blends of 10 and 30 wt. % of HyperBlocks with Kraton$^{TM}$ D-1160 was cast onto rectangular molds of polytetrafluoroethylene (PTFE) with a base of siliconised paper. SAXS experiments were performed on BM26B (DUBBLE) at the ESRF, Grenoble, France. Samples were placed in modified DSC pans and mounted in a Linkam holder. The samples were measured with the Pilatus 1M (pixel size 172 microns), the sample to detector distance was 2095 mm, the beam energy was 1.033Å. The calibration for SAXs measurements was performed using AgBe.

**Macromonomer synthesis.**

*Synthesis of Poly(styrene-isoprene-styrene) (PS-PI-PS) Triblock $AB_2$ Macromonomer.* The synthesis of the triblock copolymers was achieved using living anionic polymerization carried out under high vacuum conditions in the total absence of impurities. The amount of initiator and monomers used were varied in order to obtain a series of macromonomers differing in molecular weight and polystyrene content. The codes used for each macromonomer e.g. P(S-I-S)X_Y indicate the total molecular weight of the macromonomer as obtained by a combination of NMR and SEC (X) and the weight fraction of styrene (Y) thus P(S-I-S)65_31 is a triblock copolymer is styrene-isoprene-styrene with a total molecular weight ($M_n$) of 65 $Kgmol^{-1}$ and 31% by weight styrene. A detailed description of the key synthetic steps can be found as electronic supporting information.

**HyperBlocks synthesis.** HyperBlocks were synthesised from the $AB_2$ macromonomers using two types of coupling reaction; a Williamson coupling reaction and copper (I)-catalysed azide-alkyne 'click' reaction. Both types of reaction were carried out under an inert atmosphere and a typical procedure for each of them is reported below.

*Synthesis of HB94_30 - Williamson Coupling Reaction.* In a 250 ml flask under an inert atmosphere of nitrogen, $AB_2$ macromonomer P(S-I-S)94_30 with a bromide 'A' group (12.30 g, 0.20 mmol) and cesium carbonate (0.66 g, 2.03 mmol) were dissolved in 120 ml of THF/DMF (50:50 v/v) to form a 10% w/v solution. The reaction mixture was heated with an oil bath to 60°C and the reaction stirred with an overhead mechanical stirrer. The progress of the reaction was followed by SEC analysis and when no further increase in the molecular weight was observed, the reaction was considered to be complete. The polymer was recovered by precipitation into methanol containing a small amount of BHT antioxidant, redissolved in THF, precipitated again and dried under vacuum. HB94_30: $M_n$= 344200 g $mol^{-1}$, $M_w$= 637300 g $mol^{-1}$, Đ 1.85, Yield 99%. (SEC 0.75 ml/min)

A second reaction was carried out with P(S-I-S)94_30 (14.78 g, 0.24 mmol), $Cs_2CO_3$ (0.79 g, 2.39 mmol) and 148 ml of THF/DMF 50:50 v/v to form a 10% w/v solution at a temperature of 60°C. HB94_30: $M_n$= 384700 g mol$^{-1}$, $M_w$= 709600 g mol$^{-1}$, Đ 1.84, Yield 99%.(SEC 0.75 ml/min)

The resulting two samples were combined into a single sample by co-dissolving the two polymers in THF and the blend was recovered by precipitation. The combined sample was characterised by SEC to obtain the molecular weight distribution. HB94_30: $M_n$= 329700 g mol$^{-1}$, $M_w$= 757800 g mol$^{-1}$, Đ 2.30

*Synthesis of HB114_23 - Azide-Alkyne 'click' Reaction.* In a 250 ml flask under an inert atmosphere of nitrogen, $AB_2$ macromonomer P(S-I-S)114_23 (10.02 g, 0.23 mmol) with one azide 'A' group and two alkyne 'B' groups was dissolved in 100 ml of THF/DMF 50:50 v/v to form a 10% w/v solution. The reaction mixture was heated with an oil bath to 30°C and stirred with an overhead mechanical stirrer. To the solution was added first sodium ascorbate (0.18 g, 0.91 mmol) and then the catalyst $CuSO_4 \cdot 5H_2O$ (0.11 g, 0.44 mmol) in a few drops of water. The progress of the reaction was followed by SEC analysis. When no further increase in the molecular weight was observed, the reaction was considered to be complete. The polymer was recovered by precipitation into methanol, redissolved in THF, precipitated again and dried under vacuum. Yield 99%. HB114_23: $M_n$= 256500 g mol$^{-1}$, $M_w$= 562200 g mol$^{-1}$, Đ 2.19, Yield 98%.

A second reaction was carried out with P(S-I-S)114_23 (13.11 g, 0.30 mmol), sodium ascorbate (0.24 g, 1.21 mmol), $CuSO_4 \cdot 5H_2O$ (0.15 g, 0.60 mmol) and 100 ml of THF/DMF 50:50 v/v to form a 10% w/v solution. HB114_23: $M_n$= 142800 g mol$^{-1}$, $M_w$= 593600 g mol$^{-1}$, Đ 4.16.

The resulting two samples were blended into a single sample by co-dissolving the two polymers in THF and the blend was recovered by precipitation. The combined sample was

characterised by SEC to obtain the molecular weight distribution. HB114_23: $M_n$= 144300 g mol$^{-1}$, $M_w$= 590000 g mol$^{-1}$, Đ 4.09

**Results and Discussion**

Linear block copolymers self-organise into morphologies dictated by three main factors i.e. the Flory-Huggins interaction parameter (χ), the molecular weight and the volume fraction of the blocks constituting the block copolymers – the composition. Numerous block copolymer morphologies including domains of spheres, cylinders, lamellae and co-continuous structures such as the gyroid morphology[77,78] (Figure 2) have been predicted from theory and experimentally observed. The equilibrium behaviour for AB and ABA block copolymers has

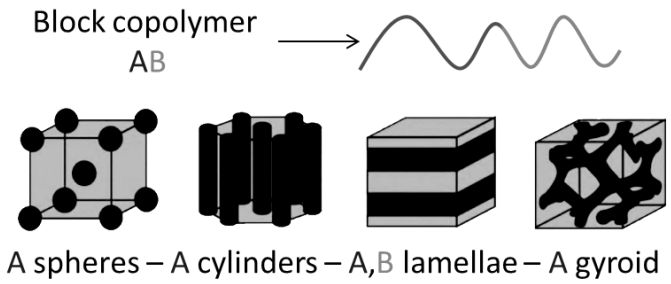


**Figure 2.** Observed morphologies for an AB diblock copolymer.

been described in detail and phase diagrams for these two types of linear copolymers have been reported by Matsen in 2000[72]. As alluded to in the introduction there is a long history of research into the impact of chain branching on solid state morphology dating back to the 1970's and more recently Matsen[79] reported equilibrium phase diagrams calculated using self-consistent field theory for a selection of two-component AB block copolymer architectures including AB, ABA, AB(AB)$_n$A linear block copolymers, AB$_2$ mikto arm stars, AB diblock multiarm stars and comb-block architectures. In all cases it was reported that the topology of the phase diagrams is relatively unaffected by differences in architecture, but the phase boundaries may shift significantly with respect to composition. Thus, well-defined morphologies are still predicted. Experimental evidence of substantial changes in

morphology has been observed in the case of nonlinear block copolymers provided with one or more branch points. Of particular note is the work of Mays *et al* who prepared graft copolymers with a polyisoprene backbone and polystyrene arms[36-38]. As a result of the synthetic strategy it was possible to prepare a series of copolymers with constant composition (volume fraction of each block) but with increasing molecular weight and number of branch points. Once again it was reported that the resulting morphologies generally agreed with theoretical predictions but in this case the extent of branching, i.e. the number of branch points, inhibited the formation of a long-range order. Samples with a low number of branch points (less than 5) showed morphologies with good long range order but as the number of branch points per chain increased the long range order was diminished. However, none of the work described above considered the impact of a hierarchical, hyperbranched architecture in which it might be expected that the higher order of branching would more dramatically influence morphology and frustrate long range order.

HyperBlocks are synthesised via a 'macromonomer' approach in a two-step procedure as illustrated in figure 3. The first step consists of the synthesis of linear macromonomers by living anionic polymerisation and the second step involves the synthesis of the hyperbranched polymers called HyperBlocks by coupling together the macromonomers.

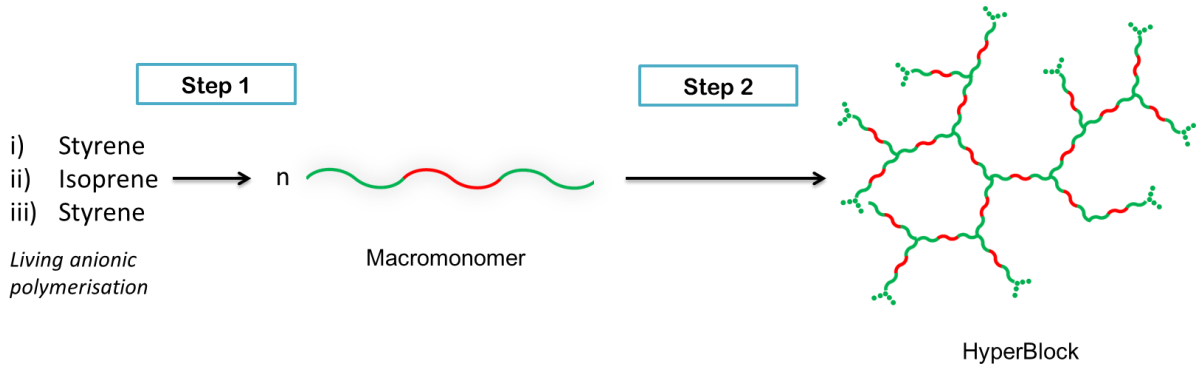


**Figure 3.** Schematic representation of the HyperBlocks synthesis via the 'macromonomer' approach using styrene and isoprene as monomers.

***Macromonomer Synthesis.*** We have previously reported the synthesis of $AB_2$ macromonomer P(S-I-S) by living anionic polymerisation and the synthesis of HyperBlocks by Williamson coupling reaction of $AB_2$ macromonomers[54]. In the current work we introduce a new way for the synthesis of HyperBlocks employing an additional type of coupling reaction, i.e. the copper (I)-catalysed azide-alkyne click reaction and produce a series of HyperBlocks from macromonomers with varying molecular weight and composition. The results in terms of molecular weight obtained from SEC and $^1$H-NMR analysis for the series of macromonomers synthesised are shown in Table 1. During the synthesis, the same amount of styrene was used for the synthesis of each of the two polystyrene blocks which therefore should have a similar block length and the triblock copolymer should be (more or less) symmetrical. The aim was to produce a set of macromonomers in which for one series, the molecular weight was held constant for varying composition and for a second series, the molecular weight was varied with constant composition.

Molecular weights were obtained by triple detection SEC using a dn/dc value of 0.185 mL/g - the dn/dc of polystyrene in THF. In this case it is possible to obtain the exact molar mass for the first PS block but the values for the PS-PI and PS-PI-PS copolymers will be inaccurate. The value of dn/dc varies depending upon the monomer and therefore copolymer composition. Since the exact composition for each sample is different, the dn/dc will also vary. For this reason the molecular weight of each sample was also calculated using $^1$H-NMR spectroscopy. The molecular weight of the first PS block was calculated by comparing the integrals of the aromatic signals of the polystyrene block and the integral of the [C**H**$_2$OSi] signal given by the initiator. These data are quoted in table 1 and are generally in very good agreement with the molecular weight obtained by SEC. However, since the [C**H**$_2$OSi] signal

**Table 1.** Molecular weight and dispersity of the first block PS, the intermediate diblock copolymer P(S-I) and the final macromonomer P(S-I-S) calculated by $^1$H-NMR spectroscopy and SEC.

| Macromonomers | PS | | | P(S-I) | | | P(S-I-S) | | |
|---|---|---|---|---|---|---|---|---|---|
| | $M_n$(g mol$^{-1}$) | | Đ | $M_n$(g mol$^{-1}$) | | Đ | $M_n$(g mol$^{-1}$) | | Đ |
| | (a) | (b) | | (a) | (b) | | (a) | (b) | |
| P(S-I-S)153_20 | 15000 | 14700 | 1.26 | 52400 | 136900 | 1.07 | 60300 | 152600 | 1.06 |
| P(S-I-S)183_20 | 17400 | 20100 | 1.24 | 81500 | 163800 | 1.04 | 93100 | 183000 | 1.04 |
| P(S-I-S)114_23 | 11700 | 14800 | 1.29 | 40100 | 99700 | 1.11 | 44400 | 113900 | 1.10 |
| P(S-I-S)94_30 | 14000 | 14400 | 1.32 | 50200 | 79600 | 1.06 | 61100 | 93900 | 1.06 |
| P(S-I-S)153_30 | 23100 | 25500 | 1.22 | 96600 | 131100 | 1.05 | 119200 | 152800 | 1.06 |
| P(S-I-S)65_31 | 9300 | 8300 | 1.24 | 26800 | 54300 | 1.06 | 33600 | 64900 | 1.05 |
| P(S-I-S)82_41 | 16000 | 17400 | 1.33 | 36600 | 64300 | 1.10 | 46300 | 81500 | 1.07 |

(a) Data obtained by SEC in THF using a value of dn/dc= 0.185mL/g

(b) Data obtained by 1H-NMR spectroscopy in $CDCl_3$ and $C_6D_6$.

from the initiator is rather weak it was decided that the data for the first PS block obtained by SEC is likely more accurate and the molecular weights of the subsequent P(S-I) and P(S-I-S) block copolymers were calculated by using the definite value of $M_n$ of the first PS block obtained by SEC and the integrals of the peaks of the aromatic protons of the polystyrene block and the integrals of the methylene protons of the polyisoprene block. Thus, the molecular weight data for the blocks obtained by NMR will be more accurate than the analogous data obtained by SEC. From the data in the table we can see that samples P(S-I-S)153_**20**, P(S-I-S)183_**20** and P(S-I-S)114_**23** all have approximately the same weight fraction of styrene (20%) but with significantly different molecular weights. Similarly there are three macromonomers with approximately 30 weight percent styrene. Of possibly greater significance is the fact that there are examples of macromonomers with nearly identical

molecular weight but varying composition; namely P(S-I-S)153_20 and P(S-I-S)153_30 which have identical molecular weights but have a 20% and 30% weigh fraction of styrene and samples P(S-I-S)114_23, P(S-I-S)94_30 and P(S-I-S)82_41 which have comparable molecular weights but weight fractions of styrene of 23%, 30% and 41% respectively.

Details of the deprotection of the alcohol functionalities and end-group modification reactions to enable both a Williamson coupling reaction and an azide-alkyne 'click' coupling reaction are described in the accompanying electronic supporting information and were carried out as previously reported[54,55,80].

***HyperBlocks synthesis via Williamson coupling reaction.*** $AB_2$ macromonomers carrying a single bromide 'A' functionality and two phenol 'B' functionalities allow the synthesis of HyperBlocks via a Williamson coupling reaction. The alkyl bromide at one end of the macromonomer chain acts as the leaving group and the phenol functionalities on the other chain end acts as the nucleophile in this reaction. The reaction conditions applied in this synthesis were developed in previously reported investigations[48,51,54] which optimised solvents, temperature, solution concentration, leaving group and type of base employed. The solvent mixture used in the present work was THF/DMF. The solution was 10% by wt. of macromonomer in THF/DMF (50/50 by volume). The use of a mixed solvent was employed to promote the polymer solvency by using THF and to favour the nucleophilc substitution by using DMF. Williamson coupling reactions are in fact promoted by aprotic solvents with high dielectric constants as, for instance, DMF (dieletric constant 36.7 at 25°C). Particular attention was paid to the purity of these solvents. THF was dried and degassed over Na/benzophenone and stored under vacuum; DMF was stored over molecular sieves. Purified solvents are necessary in Williamson coupling reaction in order to minimise any side reactions. The base cesium carbonate ($Cs_2CO_3$) was used in a molar ratio of 1:10 with respect to the macromonomer and the temperature chosen was 60°C with the exception of HB65_31

that was synthesised at 40°C for reasons explained hereafter. The progress of the coupling reaction was followed by extracting small samples periodically and subjecting them to SEC analysis as shown in Figure 4.

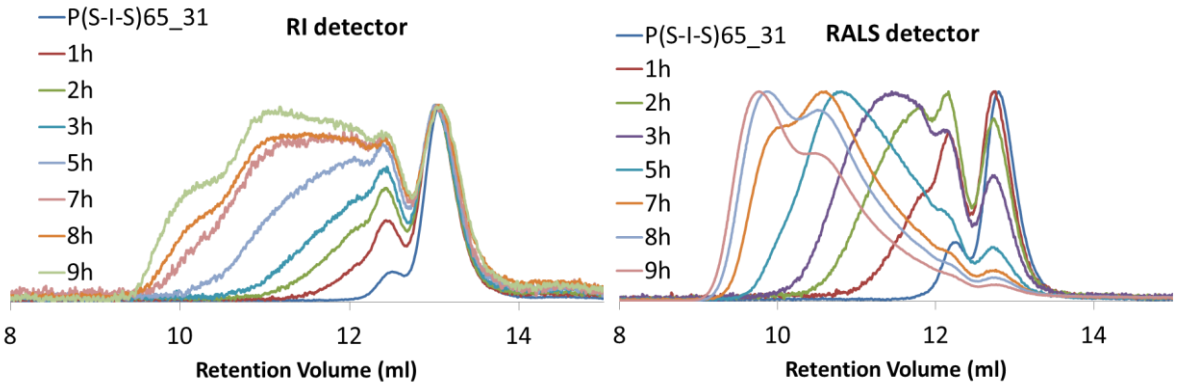


**Figure 4.** SEC chromatograms of a small scale synthesis of HyperBlock starting from the macromonomer P(S-I-S)65_31. Samples taken at different times during the reaction carried out at 40°C, 50:50 DMF/THF 10% wt/v solution.

Figure 4 shows typical refractive index (RI) and right-angle light scattering (RALS) SEC traces obtained for samples collected during the HyperBlock synthesis. On the right of each chromatogram it is possible to observe a sharp peak at a retention volume of about 13 ml corresponding to the (unreacted) macromonomer P(S-I-S)65_31. The starting macromonomer shows on the left a small peak (12.5 ml) due to the coupling of two macromonomer chains (dimer) during the termination step of the living anionic polymerisation due to the presence of environmental impurities. Observing the RI response it can be seen that the peak representing the dimer (two coupled macromonomer chains) arising from Williamson coupling is already present in significant quantity after the first hour of reaction and the extent of coupling continues to increase in each sample taken during the reaction time. That part of the distribution emerging at lower elution volumes (9.5-12.0 ml) on the left of the macromonomer peak (13 ml) represents the formation of the hyperbranched polymer, HyperBlock. The peak of the macromonomer is present in each chromatogram and indicates

that there is still uncoupled macromonomers in the reaction mixture. The presence of unreacted macromonomer could be explained in part by the presence of macromonomer which has not undergone successful end-capping with DPE-OSi although even in this case macromonomer could still be incorporated into growing HyperBlocks through the bromide group. However, in previous similar studies carried out both in our labs and others[81], residual, unreacted macromonomer is always observed. The coupling reaction of P(S-I-S)65_31 was carried out at 40°C instead of 60°C in order to slow down the rate of reaction. It was found that when this particular macromonomer was coupled at 60°C the rate of coupling was of such high efficiency that in few hours (4 h) the coupling reaction produced very high molecular weight, highly branched polymers and the resulting Hyperblock was no longer completely soluble in solvents like THF, but behaved more like a swollen gel due to the high molecular weight chains produced during the coupling. We believe that in this case the polymer is not crosslinked but has a very high molecular weight – probably with some fraction of the polymer having a molecular weight of many millions g $mol^{-1}$. This observation has been made before during the synthesis of polystyrene HyperMacs[82]. A series of HyperBlocks have been synthesised with molecular characteristics reported in Table 2. The HyperBlocks produced in this work are highly disperse in terms of both molecular weight and architecture – as expected. Each HyperBlock is characterised by a value of $Dp_n$ and $Dp_w$ that are used to describe the extent of the coupling reaction. Dp is the degree of macromonomer polymerisation and it represents the number of macromonomers reacted and coupled together to form the HyperBlocks. $Dp_n$ and $Dp_w$ are the number-average and weight-average degree of polymerisation respectively.

Each Williamson coupling reaction was carried out in duplicate in order to establish reproducibility of the reaction and in order to avoid the loss of the entire amount of material in case of oxidative degradation of the macromonomer during the reaction caused by the

**Table 2** Molecular weight data for the HyperBlocks synthesised by Williamson coupling reaction. Molecular weights calculated by SEC using dn/dc of polystyrene in THF (0.185).

| Macromonomer | HyperBlock | $M_n$ ($g \cdot mol^{-1}$) | $Dp_n$ | $M_w$ ($g \cdot mol^{-1}$) | $Dp_w$ | Đ |
|---|---|---|---|---|---|---|
| P(S-I-S)65_31 | HB65_31 | 220600 | 6.6 | 826400 | 23.3 | 3.75 |
| | HB65_31 | 218200 | 6.5 | 959000 | 27.1 | 4.40 |
| P(S-I-S)82_41 | HB82_41[(a)] | 390100 | 8.4 | 807700 | 16.3 | 2.07 |
| | HB82_41[(a)] | 354500 | 7.7 | 664800 | 13.4 | 1.88 |
| P(S-I-S)183_20 | HB183_20 | 216500 | 2.3 | 791900 | 8.2 | 3.66 |
| P(S-I-S)94_30 | HB94_30[(a)] | 344200 | 5.6 | 637300 | 9.8 | 1.85 |
| | HB94_30[(a)] | 384700 | 6.3 | 709600 | 10.9 | 1.84 |
| P(S-I-S)153_30 | HB153_30 | 453500 | 3.8 | 1007000 | 8.0 | 2.22 |

(a) Data from SEC analysis in THF at a flow rate of 0.75 ml/min.

accidental presence of oxygen in the reaction vessel. For each macromonomer the two reactions yielded very similar HyperBlocks which were subsequently solution-blended together to form a single sample of each HyperBlock. In some cases, only half of the batch of macromonomer was coupled via a Williamson coupling reaction and hence only one set of molecular weight data is presented in Table 2. In these cases, the remaining sample of macromonomer has been converted to HyperBlocks via the second type of coupling reaction, the copper (I)-catalysed azide-alkyne 'click' reaction, which will be described hereafter. A further observation that can be made when considering all of the results of coupling reactions with the different macromonomers, is that the highest degrees of coupling were obtained for HB65_31, i.e. the coupling of the macromonomer P(S-I-S)65_31 – the macromonomer with the lowest molecular weight. The degree of polymerisation ($Dp_n$ 6.6-6.5 and $Dp_w$ 23.3-27.1) and the dispersity (3.75-4.40) are higher than obtained in the coupling of the other higher molecular weight macromonomers. It is also noteworthy that although the synthesis of

HyperBlock HB65_31, proved to give the highest extent of coupling in the current study, this result is not quite as high as the HyperBlock obtained in the previous work[54]. In optimising the best conditions for the coupling reaction, Hutchings *et al*. obtained a sample of HyperBlock with $Dp_n$ 10.5 and $Dp_w$ 31.8 from a small scale reaction (1-2 g). A similar result was also obtained in the current work for HB65_31 when the coupling was carried out on a small scale (2 g) at 60 °C ($DP_n$ 10.3 and $Dp_w$ 29.6). However, the resulting polymer resembled a gel with very limited solubility as already mentioned. For this reason the reaction conditions were modified in order to obtain a readily soluble polymer and be able to stop the reaction at a lower degree of coupling. The temperature was thus decreased to 40°C. It can be seen from Table 2 that the degree of polymerisation (extent of macromonomer coupling) decreases in this order: HB65_31> HB82_41 > HB94_30 > HB153_30 ≈ HB183_20 – a trend which coincides with an increase in the molecular weight of the linear precursor of each HyperBlock. Therefore a likely explanation for the decrease in the extent of coupling reaction is the increase in molecular weight of the macromonomer. There may be two factors which support this hypothesis. Firstly, the higher molecular weight macromonomers will tend to increase the viscosity of the reaction solution, resulting in a reduction of chain mobility and less efficient stirring/poorer mixing could be responsible for the lower degree of coupling. In addition the concentration of the reactive groups A and B of the macromonomers in the reaction mixture decreases with the increase in molecular weight which results in a lower rate of reaction. The scaling up of the coupling reaction appeared to create a further problem in the synthesis of HyperBlocks, in common with the previous work, in which it was observed that scaling up (to 20 g) the coupling of the macromonomer resulted in a lower degree of coupling. The previously reported HyperBlock had a $Dp_n$ of 6.7 and a $Dp_w$ of 16.5 when produced on a 20 g scale cf. $Dp_n$ of 10.5 and a $Dp_w$ of 31.8 when coupled on a 2 g scale. In the present study this problem was minimised by carrying out reactions using a maximum of

15 g of macromonomer. This scale allowed us to maintain a similar degree of polymerisation as that obtained in the small scale reactions carried out as trial reactions.

The success of the coupling reaction can also be influenced by the extent of the end-capping reaction carried out on each macromonomers. A high degree of end-capping ensures a high concentration of $AB_2$ macromonomer chains with the required two phenol (B) groups and the bromide (A) functionality. Where the degree of end-capping with DPE-OSi is less than quantitative, macromonomers in which the B groups are absent will be present which will undoubtedly result in the production of HyperBlocks with lower degree of polymerisation. Fortunately, the efficiency of the end-capping reaction is high, subject to the absence of impurities and has been shown to be almost quantitative[48].

***HyperBlock Synthesis via copper (I)-catalysed azide-alkyne 'click' reaction***. The copper (I)-catalysed azide-alkyne 'click' reaction was s second type of coupling reaction investigated in this work for the synthesis of HyperBlocks. In this case the macromonomers are joined together by an addition reaction (Scheme 1) between the azide functionality and the alkyne functionality introduced at the chain ends during the macromonomer preparation. The

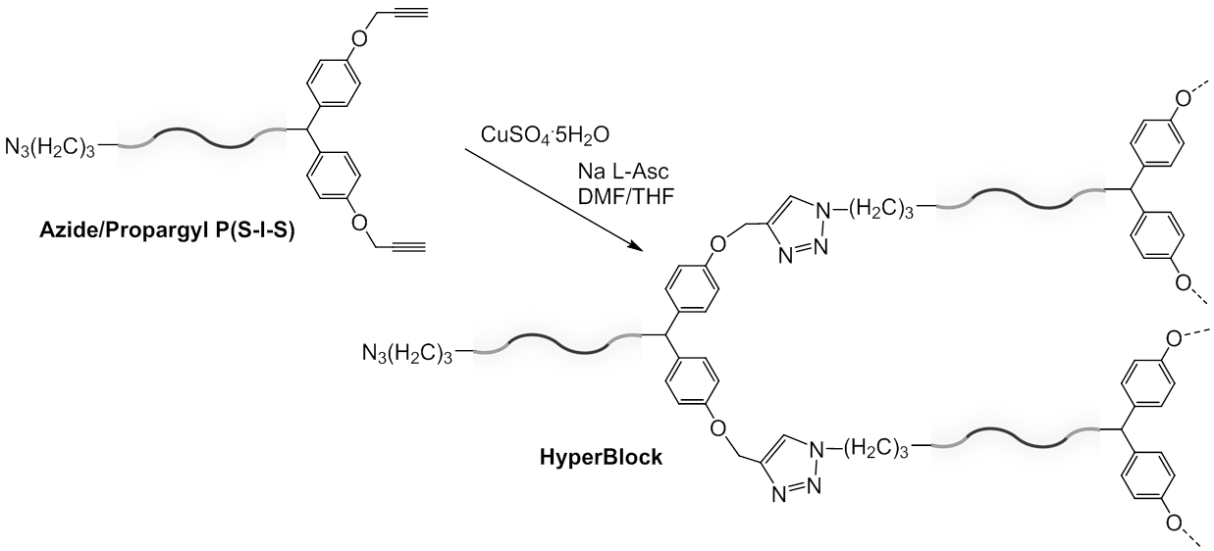


**Scheme 1.** Azide-alkyne 'click' reaction for the synthesis of HyperBlocks.

reaction leads to the formation of a 1,2,3-triazole linkage that replaces the ether linkage formed in a Williamson coupling reaction. The macromonomer was dissolved in a mixture of THF and DMF (50/50 ratio) in the presence of copper(II) sulphate pentahydrate ($CuSO_4 \cdot 5H_2O$) as the catalyst and sodium ascorbate (Na L-Asc) as the *in situ* reducing agent needed to generate the Cu(I)[67]. These two compounds were added in few drops of water which corresponded to ca. 0.8% of the solvent mixture. As was the case for the Williamson coupling reaction, the progress of the reaction was followed by the removal of samples and characterisation by SEC (table 3).

**Table 3.** Molecular weight data for HyperBlocks synthesised by azide-alkyne 'click' reaction

| Macromonomer | HyperBlock | $M_n$ ($g \cdot mol^{-1}$) | $DP_n$ | $M_w$ ($g \cdot mol^{-1}$) | $DP_w$ | Đ |
|---|---|---|---|---|---|---|
| P(S-I-S)153_20 | HB153_20 | 299900 | 5.0 | 743800 | 11.7 | 2.48 |
| | HB153_20 | 261600 | 4.3 | 677800 | 10.6 | 2.59 |
| P(S-I-S)114_23 | HB114_23 | 256500 | 5.8 | 562200 | 11.5 | 2.19 |
| | HB114_23 | 142800 | 3.2 | 593600 | 12.2 | 4.15 |
| P(S-I-S)183_20 | HB183_20 | 320600 | 3.4 | 497400 | 5.1 | 1.55 |
| P(S-I-S)153_30 | HB153_30[(a)] | 455300 | 3.8 | 661800 | 5.3 | 1.45 |

(a) Data from SEC analysis in THF at a flow rate of 0.75 ml/min.

As was observed in the case of the synthesis by Williamson coupling reaction, where two identical click coupling reactions were carried out (for both HB153_20 and HB114_23) the results were rather similar and moreover, the extent of click coupling/degree of polymerisation for these two macromonomers was comparable to the extent of coupling seen for the Williamson coupling reactions. That said the extent of coupling for HB153_30 was unexpectedly low ($DP_w$ = 5.3) compared to HB153_20 ($DP_w$ = c. 11.0) despite the two linear precursors having nearly identical molecular weights. However, a likely explanation for this discrepancy lies in the relative success of the macromonomer end-capping reactions which

was 70% and 94% for HB153_30 and HB153_20 respectively. As mentioned above in the context of Williamson coupling reactions, it is likely that solubility, macromonomer molecular weight, concentration of reactive groups A and B, reaction scale and extent of macromonomer end-capping all influence the extent of the click coupling reaction.

***HyperBlocks: a comparison between Williamson and 'click' coupling reaction***. The synthesis of HyperBlocks has been carried out utilising two different strategies; a Williamson coupling reaction and a copper (I)-catalysed azide-alkyne 'click' coupling reaction. The majority of the HyperBlocks were synthesised by Williamson coupling reaction that, thanks to optimisation achieved in a previous study, proved to be a very efficient route. HB65_31, HB82_41 and HB94_30 all showed relatively high values for the degree of polymerisation (extent of coupling) however in general, the coupling reactions showed decreasing effectiveness with increasing molecular weight of the macromonomer. Thus in an attempt to obtain polymers with higher degrees of branching from the higher molecular weight macromonomers, the widely exploited copper (I)-catalysed azide-alkyne 'click' reaction was investigated. This route for the coupling of macromonomers had been already employed to good effect in a previous study for the synthesis of asymmetric three-arm stars[55]. The 'click' coupling reaction for star polymer synthesis appeared to be more efficient and more reproducible than the Williamson coupling reaction and the ongoing popularity of using 'click' coupling reactions in the wider literature for the synthesis of branched polymers[83] convinced us to investigate this route for the synthesis of HyperBlocks. P(S-I-S)153_20 and P(S-I-S)114_23 were coupled on a large scale by 'click' coupling reaction only and the results were comparable to analogous reactions carried out using Williamson coupling reactions (Table 2 and Table 3). Macromonomers P(S-I-S)183_20 and P(S-I-S)153_30 were the only macromonomers which were coupled on a large scale by both of the two strategies. Table 4 compares the two HyperBlocks obtained by the two different coupling reactions.

**Table 4.** Comparison of molecular weight, dispersity and degree of polymerisation of HyperBlocks synthesised by Williamson and 'click' coupling reactions.

| Macromonomer | HyperBlock | $M_n$ (g·mol$^{-1}$) | $DP_n$ | $M_w$ (g·mol$^{-1}$) | $DP_w$ | Đ |
|---|---|---|---|---|---|---|
| P(S-I-S)183_20 | HB183_20[(b)] | 216500 | 2.3 | 791900 | 8.2 | 3.66 |
| | HB183_20[(c)] | 320600 | 3.4 | 497400 | 5.1 | 1.55 |
| P(S-I-S)153_30 | HB153_30[(b)] | 453500 | 3.8 | 1007000 | 8.0 | 2.22 |
| | HB153_30[(a)(c)] | 455300 | 3.8 | 661800 | 5.3 | 1.45 |

(a) Data from SEC analysis in THF at a flow rate of 0.75 ml/min.

(b) HyperBlocks synthesized by Williamson coupling reaction.

(c) HyperBlocks synthesized by azide-alkyne 'click' reaction.

It is clear from the data in table 4 that for the case of each macromonomer, the degree of polymerisation and the broader dispersity shows that somewhat better results were obtained for the HyperBlocks synthesised by Williamson coupling reaction. For both coupling reactions, in an attempt to obtain a higher extent of reaction, the macromonomers were allowed to react for a long time (between 20 and 40 hours) but prolonged reaction times did not significantly influence the outcome. Higher loadings of catalyst had proven beneficial in a previous study[55] but also made no substantive difference to the outcome in the present study.

A final series of six HyperBlocks was completed by blending together the branched polymers obtained by Williamson and/or azide-alkyne 'click' reaction. The molecular weight, degree of polymerisation and dispersity data for each single HyperBlock obtained after blending of the various batches are shown in table 5.

**Table 5.** Data for the final HyperBlocks analysed by SEC analysis by using the dn/dc of the polystyrene in THF.

| Macromonomer | HyperBlock | $M_n$ (g·mol$^{-1}$) | $DP_n$ | $M_w$ (g·mol$^{-1}$) | $DP_w$ | Đ |
|---|---|---|---|---|---|---|
| P(S-I-S)183_20 | HB183_20 | 269600 | 2.9 | 779700 | 8.1 | 2.89 |
| P(S-I-S)114_23 | HB114_23 | 144300 | 3.3 | 590000 | 12.1 | 4.09 |
| P(S-I-S)94_30 | HB94_30 | 329700 | 5.4 | 757800 | 11.7 | 2.30 |
| P(S-I-S)153_30 | HB153_30 | 398500 | 3.3 | 992100 | 7.9 | 2.49 |
| P(S-I-S)65_31 | HB65_31 | 156400 | 4.7 | 870700 | 24.6 | 5.57 |
| P(S-I-S)82_41 | HB82_41 | 308300 | 6.7 | 808500 | 16.3 | 2.62 |

**Solid-state morphology of HyperBlocks** Poly(styrene-isoprene-styrene) linear triblock copolymers and Hyperblocks were characterised by transmission electron microscopy (TEM) and small angle X-ray scattering (SAXS) to investigate the effect of the composition and branched architecture upon the solid-state morphology. The morphology of commercially available thermoplastic elastomers (TPEs) (supplied by Kraton$^{TM}$), comprising of linear and star block copolymers of PS and PI, were also explored by TEM and additional morphology studies were carried out on blends of the Kraton$^{TM}$ linear TPE with 10 and 30 wt. % of HyperBlock.

**Table 6.** Molecular characteristics of commercial TPEs from Kraton$^{TM}$ Polymers

| SEC in THF | Triple detection[a] | | | |
|---|---|---|---|---|
| ***Kraton$^{TM}$*** | **$M_n$ (g mol$^{-1}$)** | **$M_w$ (g mol$^{-1}$)** | **Đ** | **PS (%)** |
| *Linear D-1160* | 89500 | 95200 | 1.06 | ~20 |
| *Star D-1124P* | 78000 | 101400 | 1.30 | ~30 |

(a) Data obtained by using dn/dc of polystyrene (0.185)

The Kraton™ TPEs were synthesised by living anionic polymerisation of styrene and isoprene and their molecular characteristics can be found in Table 6. The two types of TPEs used were Kraton™ D-1160 which is a linear P(SIS) triblock copolymer which is similar to the macromonomers synthesised in this work, and Kraton™ D-1124P which is a three-arm star with arms of P(SI) diblock copolymers.

TEM is a microscopy technique used extensively for the analysis of block copolymer morphologies in the solid or melt state. The analysis by TEM of a small area of a sample provides directly a picture of the morphology that block copolymers adopt as a result of microphase separation. SAXS is a scattering technique used to probe the nanoscale structure and domain size of block copolymer systems among other applications[78,84]. Samples for TEM were prepared by dissolving the block copolymers (macromonomer, HyperBlocks and blends of the latter with Kraton™ linear TPE) in toluene (6% w/v for HyperBlocks and 30% w/v for macromonomers and blends) in the presence of a small quantity of the antioxidant 3,5-di-*tert*-butyl-4-hydroxytoluene (BHT). The polymer solution was subsequently poured onto circular aluminium plates of 1 mm thickness. The solvent was allowed to evaporate at room temperature for few days and then the solution cast films were dried under vacuum to constant weight. In a previously reported procedure for the sample preparation[54] an annealing step was carried out in which the films were maintained at 120°C for 7 days under vacuum in order to reach the equilibrium morphology. In the present study, a slightly different approach was used in order to understand if the annealing step was really required to equilibrate the morphology. Kraton™ D-1124P, PS-PI three-arm star, was solution cast from toluene as described above, onto two aluminium plates and dried to constant weight under vacuum. One of the samples was then annealed at 120°C under vacuum for 7 days prior the TEM analysis, whereas the other sample was analysed by TEM without any further treatments. The TEM-

micrographs of the two samples of Kraton$^{TM}$ star prepared by each method are shown below in figure 5.

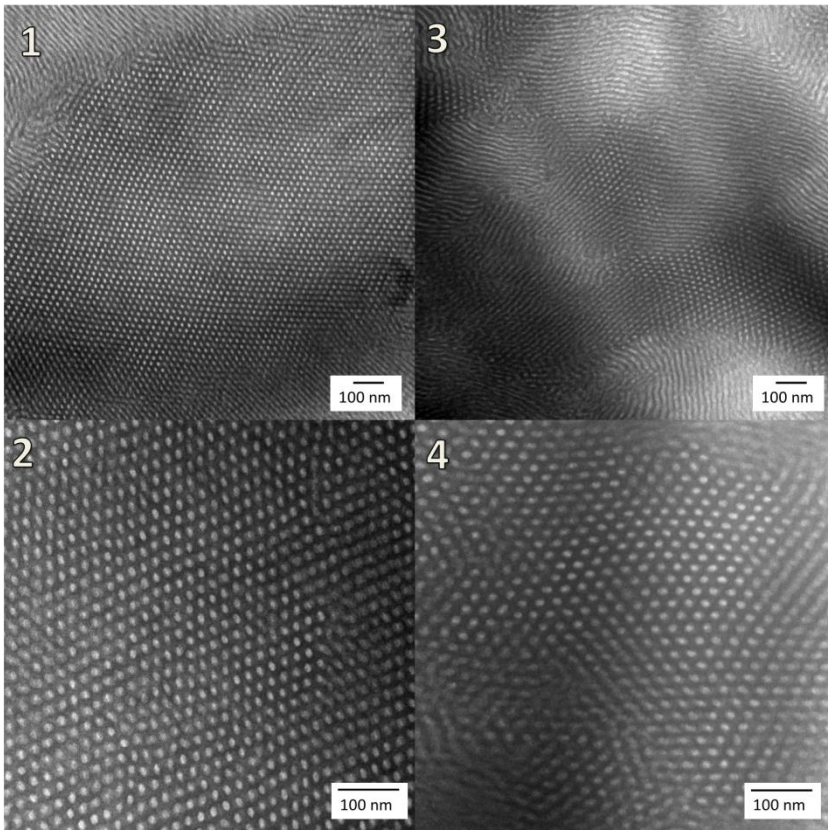


**Figure 5.** TEM micrographs of Kraton$^{TM}$ D-1124P three-arm star (30% PS). 1 and 2 are images for the unannealed film, 3 and 4 are the images for the films annealed at 120°C.

It is clear from the images in figure 5, that both the annealed (3-4) and unannealed samples (1-2) of the star-branched block copolymer are microphase separated with identical hexagonally packed cylindrical morphology. The micrographs show dark and light domains which correspond to the polyisoprene and polystyrene blocks respectively. The dark colour arises by exposing the film to osmium tetraoxide ($OsO_4$) vapour, which stains the unsaturated rubbery component (PI) but not the glassy component (PS). The cylindrical morphology is indicated by the coexistence of both the cylinders "end-on" appearing as circular domains and transverse ("side-on") segments of polystyrene cylinders in the polyisoprene matrix. From these images it seems that the solvent-casting technique of sample preparation is more

than adequate to enable the Kraton three-arm star copolymer to reach its equilibrium morphology without the need of the annealing step. It is accepted that the HyperBlock copolymers are higher molecular weight than the Kraton three-arm star and that it is expected that the extremely high molecular weights and highly branched architecture might result exceptionally high barriers to macromolecular reorganization, possibly leading to the observation of kinetically trapped morphologies in HyperBlocks. However, it is worth noting that in the previous proof of principle study, the additional annealing step of seven days at 120 $^{o}$C (above the $T_g$ for polystyrene) did not reveal any difference in morphology to those observed in the current study and described below. Whether the described morphologies are equilibrium or kinetically trapped is unclear but it is clear that the HyperBlock morphologies do not appear to change with prolonged annealing.

*Morphology of Linear Macromonomers.* The morphology of each linear ABA macromonomer has been determined and allows a systematic evaluation to be made of the impact of composition and molecular weight upon morphology.

Polymers such as the linear ABA triblock copolymers synthesised in this work have hard/glassy blocks at each end of the polymer chains (polystyrene) and a soft/rubbery block in the inner part (polyisoprene block). The macromonomer structure can be schematically represented as in figure 6 where the blocks at each end of the chain have similar molecular weights and the inner block constitutes the larger part of the linear chain.

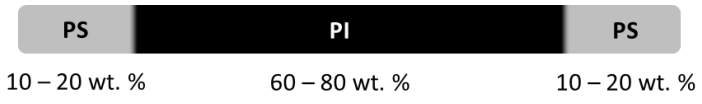


**Figure 6.** Schematic representation of linear macromonomers P(S-I-S). The weight percentage of each polystyrene block varies from 10 to 20 wt. % and from 60 to 80 wt. % for the polyisoprene block.

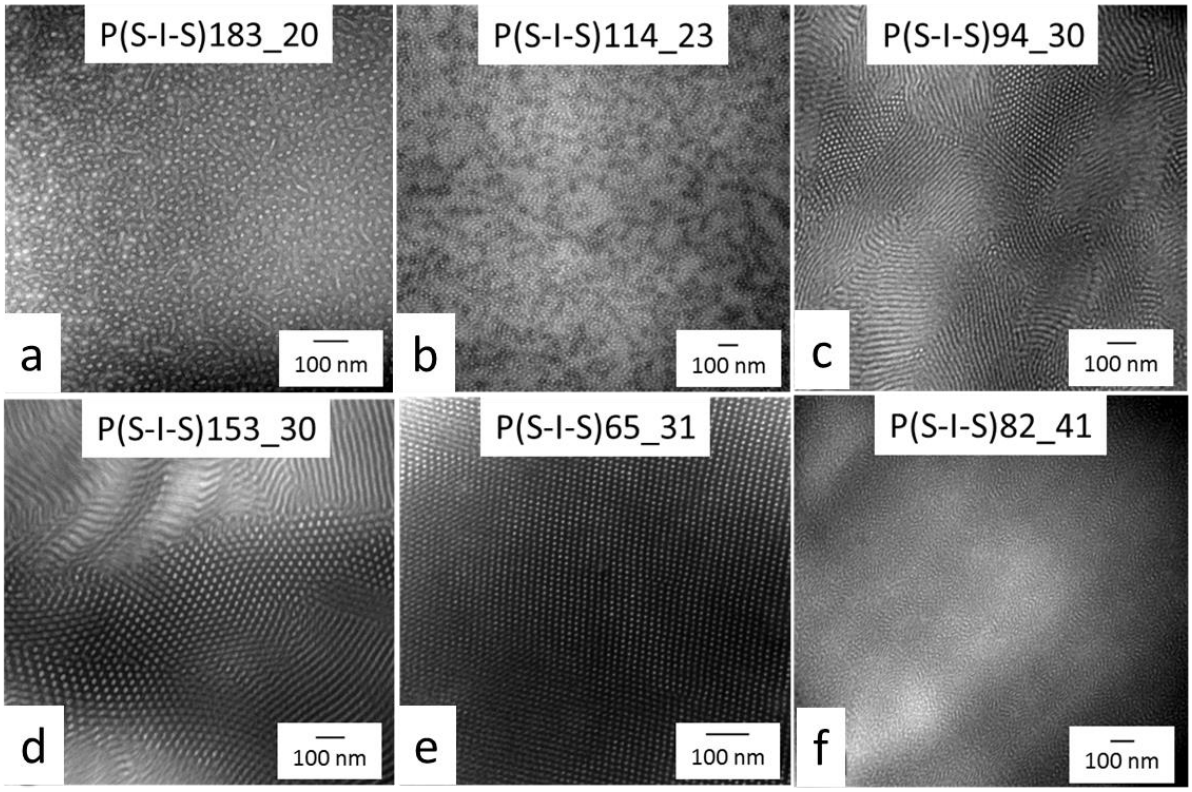


**Figure 7.** TEM micrographs of linear ABA triblock copolymer macromonomers

As expected, changes in the molecular weight and polystyrene weight fraction results in different morphologies for the linear P(S-I-S) triblock copolymers. The TEM images presented in figure 7 illustrate how the morphology of the ABA triblock copolymer macromonomers varies by changing the molecular weight and the weight fraction of polystyrene. P(S-I-S)94_30, P(S-I-S)153_30 and P(S-I-S)65_31 (Figure 7c, d and e) with a content of polystyrene of 30 wt. % all show a cylindrical morphology. In the TEM images it is possible to identify hexagonally packed cylinders in both side-on and head-on orientations. These three images are similar to the TEM images for Kraton$^{TM}$ D-1124P (Figure 4) which is a star-branched polymer with a similar content of polystyrene c 30 wt. % and also shows a cylindrical morphology – in the case of Kraton$^{TM}$ D-1124P, the star-branched architecture has no demonstrable impact on morphology in line with previous reports[79]. The change in molecular weight does not seem to affect the morphology of the macromonomers with 30 wt.

% of polystyrene; however the molecular weight does have an impact on the domain sizes as expected. It can be seen that by decreasing the molecular weight of the macromonomer, the domain size of polystyrene cylinders get smaller. This is particular evident by comparing Figure 8d and 8e where the measured domain sizes (cylinder diameter) are approximately 17 nm and 8 nm respectively for styrene block lengths of approximately 23,000 $gmol^{-1}$ and 9,500 $gmol^{-1}$ respectively (table 1). The cylindrical morphology of P(S-I-S)153_30 and P(S-I-S)65_31 are confirmed by SAXS analysis that shows scattering curves with at least four reflections. (Figure 8)

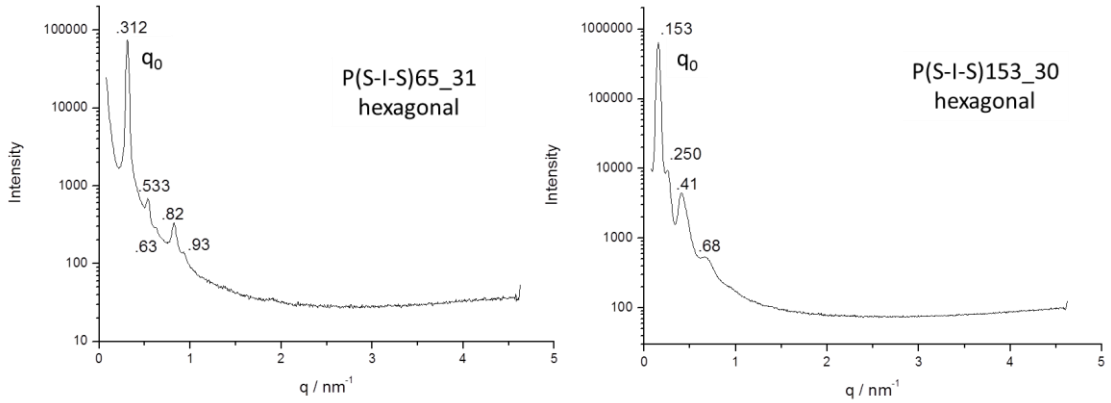


**Figure 8.** SAXS curves: Intensity versus scattering vector q for P(S-I-S)65_31 and P(S-I-S)153_30.

The two SAXS-profiles show the presence of one significant scattering maximum corresponding to $q_0$ (at 0.312 and 0.153 $nm^{-1}$) and indicating the presence of phase separation. Higher-order reflections with peak position ratios of 1:√3:2:√7:3 and 1:√3:√7:√20 respectively for P(S-I-S)65_31 and P(S-I-S)153_30 indicate a morphology of hexagonally packed cylinders with long range order for both the samples.

Macromonomers P(S-I-S)183_20 and P(S-I-S)114_23 (figure 7a and 7b) have a lower polystyrene content (20 wt. %) and they show a morphology which is more spherical in nature although the morphology is not perfect and it is possible that at 20% styrene these samples lie close to a morphology phase boundary[78,84]. The increase in styrene weight

fraction to a little over 40 wt% in P(S-I-S)82_41 results in a less well-ordered morphology. The segregation in microphases is still visible but the long-range order is less obvious.

*HyperBlocks morphology*. A dramatic change in the morphology is noticed when the macromonomers are converted into HyperBlocks and branch points are introduced. Figure 9 shows the TEM micrographs of the HyperBlocks synthesised from each of the macromonomers mentioned above.

The comparison of the two sets of TEM images, macromonomers and HyperBlocks, in Figure 7 and 9 respectively shows the changes in the morphology of the triblock copolymers

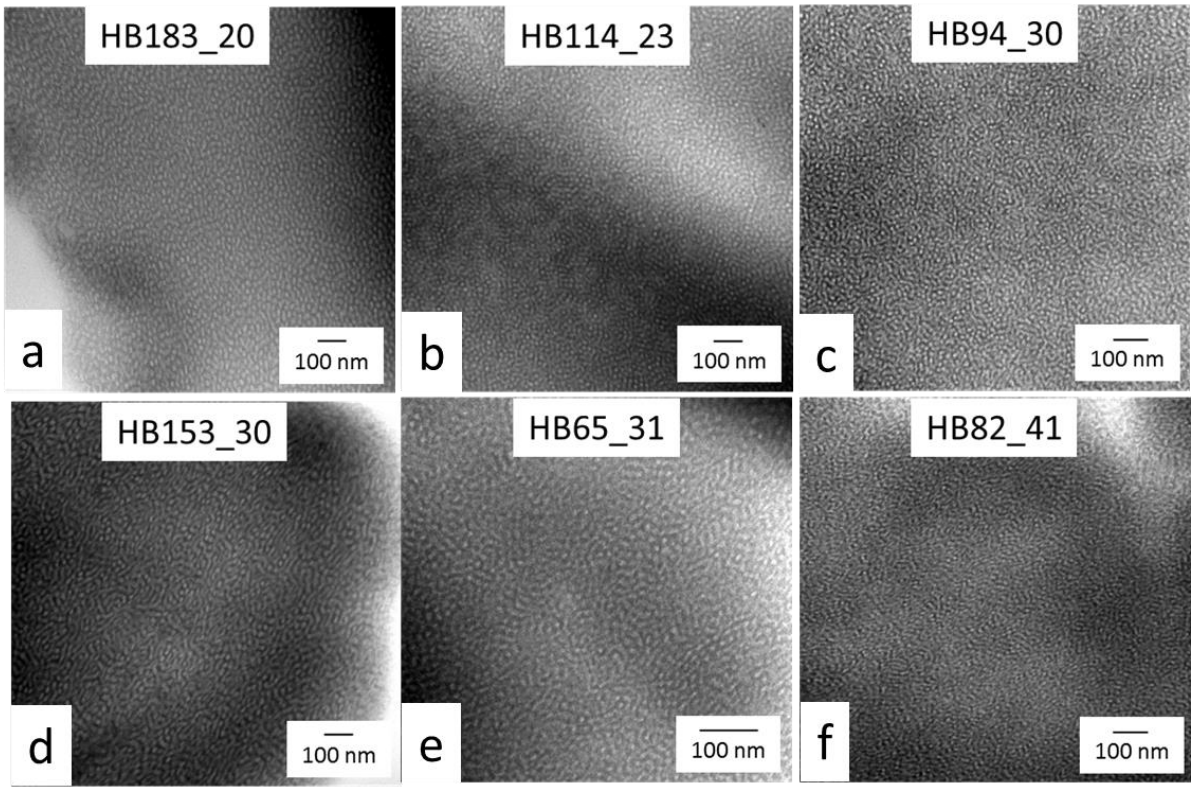


**Figure 9.** TEM micrographs of HyperBlocks

due to the transformation of the architecture from linear to branched. The change of the architecture clearly has a dramatic effect on the self-assembly of the block copolymers. Each image shows that the HyperBlocks are microphase separated but in each case the HyperBlocks lack any long-range order. The composition of each HyperBlock is identical to

the precursor macromonomer and the absence of any long-range order must therefore due to the complex branched architecture of the HyperBlocks. The effect of branching points on morphology has been previously reported by Mays *et al*. and discussed above, in the case of graft copolymers made with polystyrene arms and a polyisoprene backbone[36-38]. It was reported that the long-range order of the graft copolymers decreased with the increase of the number of branch points at the same volume fraction of polystyrene, leading to morphologies similar to the ones reported in this work. In addition the results reported herein are consistent with result obtained previously by Hutchings[54] where a similar change in morphology was observed accompanying the transformation of the macromonomer into HyperBlock. In the current study, the contrast in morphology between linear precursor and branched HyperBlock is most obvious for the samples in which the styrene content is approximately 30% by weight where the long-range order is strongest in the macromonomer. Thus, significant changes to the observed morphology of the macromonomer can be observed for the HyperBlocks HB94_30, HB153_30 and HB65_31. The well-defined, long-range order in the cylindrical morphology of the corresponding macromonomers is lost and the microphase separation, whilst still visible, lacks long-range lattice order. HB153_30 and HB65_31 were also analysed by SAXS which supports the presence of microphase separation in these samples (Figure 10). The presence of two features for each sample could suggest that these samples have some longer range lattice order but equally does not confirm any lattice order. These features could also be correlation hole scattering with weak form factor oscillations consistent with microphase separation lacking any order whatsoever, which in turn is consistent with the TEM images.

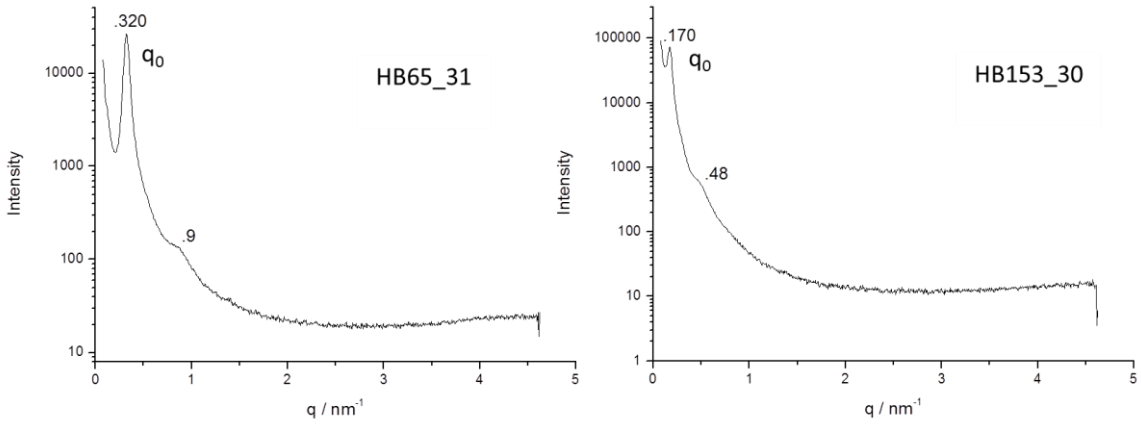


**Figure 10.** SAXS data for samples HB153_30 and HB65_31.

The SAXS curves exhibit strong primary reflection $q_0$ (0.320 and 0.170 $nm^{-1}$) but there are fewer higher-order reflections and they are broader and much weaker than those observed for the precursor macromonomers (Figure 8), consistent with a reduction in long-range lattice order. The higher order peak for both samples is close to √8q0 which although consistent with cubic order[78,84] this feature could be also be due to form factor oscillations and does not lead us to suspect anything other than a disordered phase. In the case of the macromonomers/HyperBlocks with a weight fraction of polystyrene of approximately 0.2 (figure 7 and 9) the impact of the branching upon morphology is less obvious. Moreover, the change of morphology for P(S-I-S)82_41 following conversion to the HyperBlock HB82_41 can be hardly detected. This is more a consequence of the macromonomer having a less ordered morphology, than the branched architecture having no impact. What can be said with certainty is that in all of the above cases, regardless of the composition or molecular weight of the linear macromonomer precursor, the resulting HyperBlocks all show microphase separation but the morphology in each case is characterised by an absence of long-range lattice order. It appears as if the branched architecture hinders the development of defined long-range lattice order, although there is still microphase separation and some local ordering in the HyperBlocks irrespective of the composition of the block copolymer.

*Morphology of Blends of Linear and Hyperbranched Block Copolymers*. Polymer blends are new materials obtained from a mixture of two or more existing polymers and they are characterised by physical properties which differ from the properties of each component. Blends are often produced in order to create materials with unique properties developed in

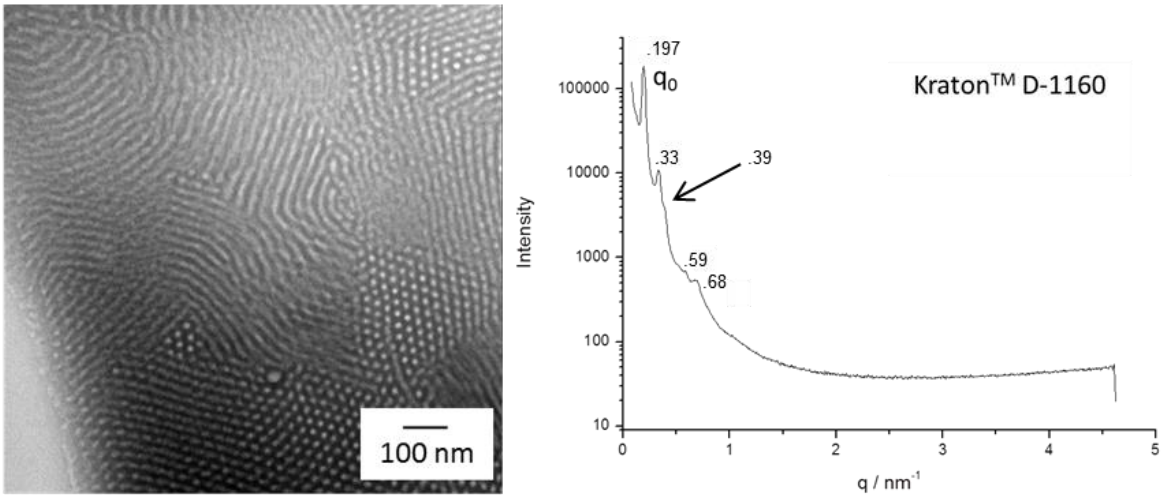


**Figure 11.** TEM micrograph and SAXS data for commercial linear TPE Kraton™ D-1160.

accordance to the applications of the material itself. We have seen above the dramatic impact that the complex branched architecture has on the morphology of HyperBlocks and it considered interesting to investigate whether the architecture of HyperBlocks would in any way impact upon the morphology of linear block copolymers when the HyperBlock was added as the minor component in a blend. The blends produced in this work were binary blends of various HyperBlocks with Kraton™ TPE (D-1160) - a commercial linear PS-PI-PS triblock copolymer. Pure Kraton™ D-1160 shows a cylindrical morphology with long-range order as evidenced by the TEM micrograph. The SAXS data is also consistent with hexagonal-packed cylindrical order, showing a series of peaks with a strong primary reflection, $q_0$ at 0.197 $nm^{-1}$, and higher order reflections at peak position ratios of 1:√3:2:3:√12 (Figure 11). In the current work, the blends were prepared by co-dissolution (in

toluene) of the Kraton$^{TM}$ D-1160 with the relevant HyperBlock. Blends containing 10% and 30% by weight of HyperBlock were prepared and the phase-separated morphology of blends of each was investigated by TEM and SAXS. It should be pointed out that given the chemical and compositional similarity of the two blend components macrophase separation was neither expected nor observed. The impact of the blend composition and specifically the impact of the presence of HyperBlock as the minor blend component upon the morphology of Kraton$^{TM}$ D-1160, the major blend component, can clearly be seen by comparing the TEM micrographs of pure Kraton$^{TM}$ D-1160 (Figure 11) and the morphology observed for each HyperBlock/Kraton$^{TM}$ D-1160 blend prepared and reported in figure 12. Figure 12 shows the TEM micrographs of blends containing each of the six HyperBlocks detailed in table 5 and discussed above. In each case blends were prepared containing 10 wt. % and 30 wt. % HyperBlock respectively. In all cases, without exception, the very well-defined, long-range order exhibited by the pure Kraton$^{TM}$ D-1160 (Figure 11) is not observed in the TEM images of the blends. In some cases, the blends containing 10 wt. % HyperBlock, notably HB183_20, HB114_23 and HB82_41, showed regions or patches of retained long range order but there was little or no vestigial long range order in blends containing 30% HyperBlock. This demonstrates that the presence of relatively small amounts of HyperBlock (10% in some cases and < 30% in all cases) in a blend with a linear copolymer of the same or very similar chemical composition influences and frustrates the formation of a morphology with well-defined, long-range lattice order. The typical morphology of the linear block polymer – hexagonally packed cylinders in this case – which is the major component of the blends, is in fact, completely lost. It is as if the presence of the HyperBlock – even as a minor component – can impose upon the blend, the same phase-separated morphology, lacking in long-range lattice order that we observe for a pure HyperBlock. These conclusions are further supported

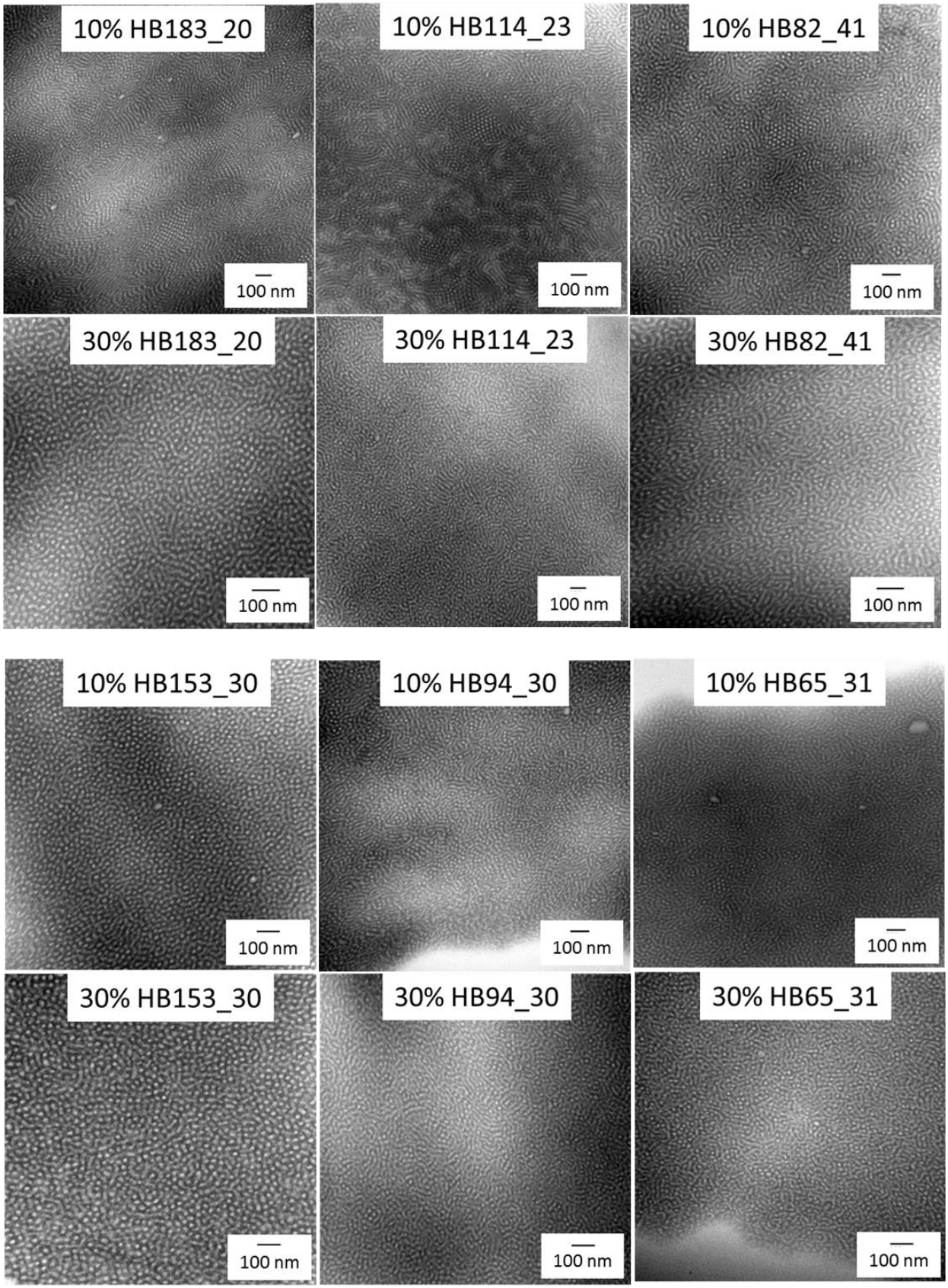


**Figure 12**. TEM micrographs of binary blends of HyperBlocks and KratonTM D-1160. Each blend contains either 10 wt. % or 30 wt. % HyperBlock.

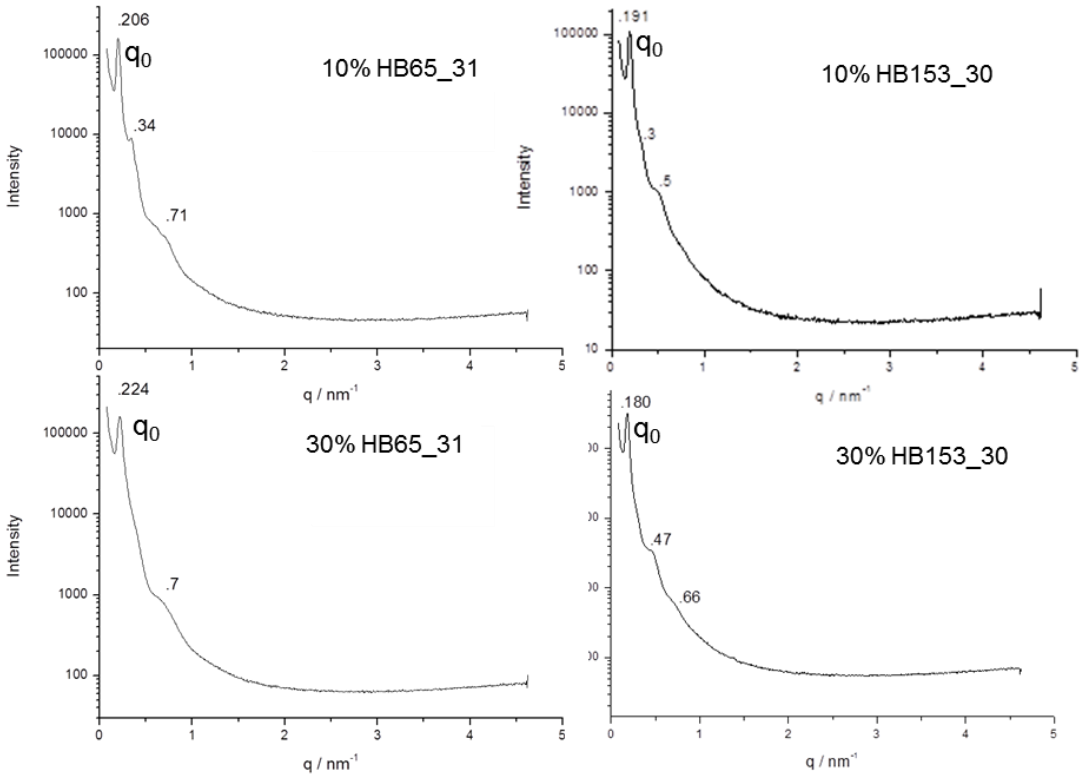


**Figure 13.** SAXS data for blends of 10% and 30% of Hyperblocks HB65_31 and HB153_30 with commercial TPE Kraton$^{TM}$ D-1160.

by SAXS analysis on the blends containing 10% and 30% of HyperBlocks HB153_30 and HB65_31 – see figure 13. SAXS analysis of pure Kraton$^{TM}$ D-1160 (Figure 11) shows a series of peaks with a strong primary reflection, $q_0$, at 0.197 nm$^{-1}$ confirming the presence of a cylindrical morphology, with long-range order, as discussed above. A primary reflection $q_0$ indicating phase separation in the blends can be observed for each set of SAXS data in figure 13, along with higher order reflections. However, the scattering profiles indicate decreasing long-range order with increasing content of HyperBlock in the blend. The SAXS data for the blend with 30% of HB65_31 cannot be indexed unambiguously, although there is a feature at higher q which may be a broad structure factor peak or a form factor peak. However, the data for the blend containing 10% HB65_31 can be indexed to a hexagonal packed cylindrical

morphology with (weak) peaks at 0.206, 0.34 and 0.71 $nm^{-1}$. In the case of the two blends of HB153_30, the SAXS data shows broad higher order peaks, again consistent with microphase separation and local lattice order and diminished long range order meaning that again, the peaks cannot be indexed unambiguously.

**Conclusions**

We have described here the synthesis of a series of hyperbranched polymers – HyperBlocks – prepared via the 'macromonomer' approach. Using this approach several $AB_2$ macromonomers of ABA triblock copolymers of polystyrene-polyisoprene-polystyrene have been prepared via living anionic polymerisation, which allows maximum control in terms of molecular weight, dispersity, microstructure and composition. Macromonomers we prepared with a varying weight fraction of polystyrene (from 20 to 41 wt. %) and a varying molecular weight (from ca. 65000 to 183000 $gmol^{-1}$). We have shown that the conversion of the linear macromonomers into HyperBlocks can be achieved efficiently by both Williamson coupling reaction and the azide-alkyne 'click' reaction. We reported the chemical modification of the end groups of the $AB_2$ macromonomers, carried out in order to obtain the suitable end group functionalities to facilitate each class of coupling reactions. The protected primary alcohol functionality was deprotected and converted into a bromide group and then to an azide group. The protected phenol functionalities were deprotected and converted to alkyne functionalities. The Williamson coupling reaction proved once again to be a very good strategy for the synthesis of hyperbranched polymers; the 'click' coupling reaction surprisingly gave slightly lower values of degree of polymerisation (extent of macromonomer coupling) and the additional two steps for the conversion of the chain-end functionalities of the macromonomers make this type of coupling less appealing for the synthesis of HyperBlocks. As expected, HyperBlocks synthesised by the two different types of coupling reactions were highly disperse in terms of molecular weight and molecular architecture.

Investigations into the solid state morphology of the resulting polymers, and in particular, the impact of the hyperbranched architecture on morphology was carried out by using both TEM and SAXS. The study of the solid-state morphology of the linear macromonomers (PS-PI-PS triblock copolymers) showed microphase separation into different morphologies in broad agreement with the theoretical predictions for linear ABA triblock copolymers morphology. By varying the content of polystyrene it was possible to observe spherical-like morphologies [P(S-I-S)183_20 and P(S-I-S)114_23] and cylindrical morphologies [P(S-I-S)94_30, P(S-I-S)153_30 and P(S-I-S)65_31] although the long range order was more well-defined in some cases than others. It was found that the conversion of these linear macromonomers to the highly branched block copolymers, HyperBlocks, resulted in the loss of the long-range, well-ordered morphologies associated with the macromonomers. The highly branched architecture of the HyperBlocks is undoubtedly the factor responsible for frustration and inhibition of the long range lattice order. The effect of the branched architecture of the HyperBlocks on the solid-state morphology was also observed in blends of Kraton$^{TM}$ D-1160 with 10 or 30 wt. % of HyperBlock whereby the presence of even small amounts (10%) of HyperBlock in these blends dramatically influences and frustrates the formation of the well-defined cylindrical morphology which is characteristic of Kraton$^{TM}$ D-1160.

**Acknowledgments**

This work was carried out as part of the EU funded Marie Curie Initial Training Network ‘‘DYNACOP’’ under the FP7 Framework and we acknowledge the financial support. TEM measurements were carried out in collaboration with Dr. Christine Richardson, School of Biological and Biomedical Sciences, Microscopy & Bioimaging at Durham University.

**References**


1. Adams, C. H.; Hutchings, L. R.; Klein, P. G.; McLeish, T. C. B.; Richards, R. W., *Macromolecules* **1996,** *29* (17), 5717-5722.
2. Frischknecht, A. L.; Milner, S. T.; Pryke, A.; Young, R. N.; Hawkins, R.; McLeish, T. C. B., *Macromolecules* **2002,** *35* (12), 4801-4820.
3. Zamponi, M.; Pyckhout-Hintzen, W.; Wischnewski, A.; Monkenbusch, M.; Willner, L.; Kali, G.; Richter, D., *Macromolecules* **2010,** *43* (1), 518-524.
4. Lee, J. H.; Goldberg, J. M.; Fetters, L. J.; Archer, L. A., *Macromolecules* **2006,** *39* (19), 6677-6685.
5. Clarke, N.; Colley, F. R.; Collins, S. A.; Hutchings, L. R.; Thompson, R. L., *Macromolecules* **2006,** *39* (3), 1290-1296.
6. Hadjichristidis, N., *Journal of Polymer Science Part a-Polymer Chemistry* **1999,** *37* (7), 857-871.
7. Hutchings, L. R.; Richards, R. W., *Polymer Bulletin* **1998,** *41* (3), 283-289.
8. Fernyhough, C. M.; Young, R. N.; Ryan, A. J.; Hutchings, L. R., *Polymer* **2006,** *47* (10), 3455-3463.
9. Iatrou, H.; Mays, J. W.; Hadjichristidis, N *Macromolecules* **1998,** *31* (19), 6697-6701.
10. Paraskeva, S.; Hadjichristidis, N., *Journal of Polymer Science Part a-Polymer Chemistry* **2000,** *38* (6), 931-935.
11. Chambon, P.; Fernyhough, C. M.; Im, K.; Chang, T.; Das, C.; Embery, J.; McLeish, T. C. B.; Read, D. J., *Macromolecules* **2008,** *41* (15), 5869-5875.
12. Hirao, A.; Murao, K.; Abouelmagd, A.; Uematsu, M.; Ito, S.; Goseki, R.; Ishizone, T., *Macromolecules* **2011,** *44* (9), 3302-3311.
13. Hirao, A.; Uematsu, M.; Kurokawa, R.; Ishizone, T.; Sugiyama, K., *Macromolecules* **2011,** *44* (14), 5638-5649.

14. McLeish, T. C. B.; Allgaier, J.; Bick, D. K.; Bishko, G.; Biswas, P.; Blackwell, R.; Blottiere, B.; Clarke, N.; Gibbs, B.; Groves, D. J.; Hakiki, A.; Heenan, R. K.; Johnson, J. M.; Kant, R.; Read, D. J.; Young, R. N., *Macromolecules* **1999,** *32* (20), 6734-6758.

15. Rahman, M. S.; Aggarwal, R.; Larson, R. G.; Dealy, J. M.; Mays, J., *Macromolecules* **2008,** *41* (21), 8225-8230.

16. Chen, X.; Rahman, M. S.; Lee, H.; Mays, J.; Chang, T.; Larson, R., *Macromolecules* **2011,** *44* (19), 7799-7809.

17. Rahman, M. S.; Lee, H.; Chen, X.; Chang, T.; Larson, R.; Mays, J., *ACS Macro Lett.* **2012,** *1* (5), 537-540.

18. Orfanou, K.; Iatrou, H.; Lohse, D. J.; Hadjichristidis, N., *Macromolecules* **2006,** *39* (13), 4361-4365.

19. Hutchings, L. R.; Roberts-Bleming, S. J., *Macromolecules* **2006,** *39* (6), 2144-2152.

20. Watanabe, H.; Matsumiya, Y.; van Ruymbeke, E.; Vlassopoulos, D.; Hadjichristidis, N., *Macromolecules* **2008,** *41* (16), 6110-6124.

21. Kimani, S. M.; Hutchings, L. R., *Macromolecular Rapid Communications* **2008,** *29* (8), 633-637.

22. Hirao, A.; Watanabe, T.; Ishizu, K.; Ree, M.; Jin, S.; Jin, K. S.; Deffieux, A.; Schappacher, M.; Carlotti, S., *Macromolecules* **2009,** *42* (3), 682-693.

23. Yoo, H. S.; Watanabe, T.; Hirao, A., *Macromolecules* **2009,** *42* (13), 4558-4570.

24. Hirao, A.; Yoo, H. S., *Polymer Journal* **2011,** *43* (1), 2-17.

25. Zhang, H. F.; He, J. P.; Zhang, C.; Ju, Z. H.; Li, J.; Yang, Y. L., *Macromolecules* **2012,** *45* (2), 828-841.

26. Hutchings, L. R.; Kimani, S. M.; Hoyle, D. M.; Read, D. J.; Das, C.; McLeish, T. C. B.; Chang, T.; Lee, H.; Auhl, D., *ACS Macro Lett.* **2012,** *1* (3), 404-408.

27. Ge, X. S.; He, C.; He, W. D.; Chen, S. Q., *Polymer Chemistry* **2014,** *5* (16), 4649-4657.

28. Zhang, C.; He, J. P., *Australian Journal of Chemistry* **2014,** *67* (1), 31-38.

29. Price, C.; Watson, A. G.; Chow, M. T., *Polymer* **1972**, *13* (7), 333-336

30. Tselikas, Y.; Hadjichristidis, N.; Lescanec, R. L.; Honeker, C. C.; Wohlgemuth, M.; Thomas, E. L., *Macromolecules* **1996,** *29* (10), 3390-3396.

31. Milner, S. T., *Macromolecules* **1994,** *27* (8), 2333-2335.

32. Hadjichristidis, N.; Iatrou, H.; Behal, S. K.; Chludzinski, J. J.; Disko, M. M.; Garner, R. T.; Liang, K. S.; Lohse, D. J.; Milner, S. T., *Macromolecules* **1993,** *26* (21), 5812-5815.

33. Tselikas, Y.; Iatrou, H.; Hadjichristidis, N.; Liang, K. S.; Mohanty, K.; Lohse, D. J., *J. Chem. Phys.* **1996,** *105* (6), 2456-2462.

34. Ishizu, K.; Uchida, S., *Prog. Polym. Sci.* **1999,** *24* (10), 1439-1480.

35. Pitsikalis, M.; Pispas, S.; Mays, J. W.; Hadjichristidis, N., *Advances in Polymer Science* **1998,** *135*, 1-137.

36. Beyer, F. L.; Gido, S. P.; Buschl, C.; Iatrou, H.; Uhrig, D.; Mays, J. W.; Chang, M. Y.; Garetz, B. A.; Balsara, N. P.; Tan, N. B.; Hadjichristidis, N. *Macromolecules* **2000,** *33*, 2039-2048.

37. Zhu, Y. Q.; Burgaz, E.; Gido, S. P.; Staudinger, U.; Weidisch, R.; Uhrig, D.; Mays, J. W. *Macromolecules* **2006,** *39*, 4428-4436.

38. Duan, Y. X.; Thunga, M.; Schlegel, R.; Sehneider, K.; Rettler, E.; Weidisch, R.; Siesler, H. W.; Stamm, M.; Mays, J. W.; Hadjichristidis, N., *Macromolecules* **2009,** *42* (12), 4155-4164.

39. Konkolewicz, D.; Monteiro, M. J.; Perrier, S., *Macromolecules* **2011,** *44* (18), 7067-7087.

40. Frechet, J. M. J.; Henmi, M.; Gitsov, I.; Aoshima, S.; Leduc, M. R.; Grubbs, R. B., *Science* **1995,** *269* (5227), 1080-1083.

41. Rikkou-Kalourkoti, M.; Matyjaszewski, K.; Patrickios, C. S. *Macromolecules* **2012**, *45*, 1313-1320.

42. Han, J.; Li, S.; Tang, A.; Gao, C. *Macromolecules* **2012**, *45*, 4966-4977.

43. Li, S.; Han, J.; Gao, C. *Polym. Chem.* **2013**, *4*, 1774-1787.

44. O'Brien, N.; McKee, A.; Sherrington, D. C.; Slark, A. T.; Titterton, A., *Polymer* **2000,** *41* (15), 6027-6031.

45. Knauss, D. M.; Al-Muallem, H. A., *Journal of Polymer Science Part a-Polymer Chemistry* **2000,** *38* (23), 4289-4298.

46. Knauss, D. M.; Al-Muallem, H. A.; Huang, T. Z.; Wu, D. T., *Macromolecules* **2000,** *33* (10), 3557-3568.

47. Al-Muallem, H. A.; Knauss, D. M., *Journal of Polymer Science Part a-Polymer Chemistry* **2001,** *39* (20), 3547-3555.

48. Hutchings, L. R.; Dodds, J. M.; Roberts-Bleming, S. J., *Macromolecules* **2005,** *38* (14), 5970-5980.

49. Hutchings, L. R.; Dodds, J. M.; Roberts-Bleming, S. J., *Macromol. Symp.* **2006,** *240*, 56-67.

50. Dodds, J. M.; De Luca, E.; Hutchings, L. R.; Clarke, N., *J. Polym. Sci. Pt. B-Polym. Phys.* **2007,** *45* (19), 2762-2769.

51. Clarke, N.; De Luca, E.; Dodds, J. M.; Kimani, S. M.; Hutchings, L. R., *Eur. Polym. J.* **2008,** *44* (3), 665-676.

52. Trollsas, M.; Atthoff, B.; Claesson, H.; Hedrick, J. L., *Macromolecules* **1998,** *31* (11), 3439-3445.

53. Trollsas, M.; Hedrick, J. L., *Macromolecules* **1998,** *31* (13), 4390-4395.

54. Hutchings, L. R.; Dodds, J. M.; Rees, D.; Kimani, S. M.; Wu, J. J.; Smith, E., *Macromolecules* **2009,** *42* (22), 8675-8687.

55. Agostini, S.; Hutchings, L. R., *Eur. Polym. J.* **2013,** *49* (9), 2769-2784.

56. Ding, L.; An, J.; Zhu, Z. S., *Polymer Chemistry* **2014,** *5* (3), 733-742.

57. Ding, L.; Qiu, J.; Zhu, Z. S., *Macromolecular Rapid Communications* **2013,** *34* (20), 1635-1641.

58. Ding, L. A.; Xie, M. R.; Yang, D.; Song, C. M., *Macromolecules* **2010,** *43* (24), 10336-10342.

59. Hilf, S.; Wurm, F.; Kilbinger, A. F. M., *Journal of Polymer Science Part a-Polymer Chemistry* **2009,** *47* (24), 6932-6940.

60. Barbey, R.; Perrier, S., *Macromolecules* **2014,** *47* (19), 6697-6705.

61. Konkolewicz, D.; Poon, C. K.; Gray-Weale, A.; Perrier, S., *Chemical Communications* **2011,** *47* (1), 239-241.

62. Li, L. W.; Wang, X.; Yang, J. X.; Ye, X. D.; Wu, C., *Macromolecules* **2014,** *47* (2), 650-658.

63. Li, L. W.; Zhou, J. F.; Wu, C., *Macromolecules* **2012,** *45* (23), 9391-9399.

64. Li, L. W.; He, C.; He, W. D.; Wu, C., *Macromolecules* **2011,** *44* (20), 8195-8206.

65. Kong, L. Z.; Sun, M.; Qiao, H. M.; Pan, C. Y., *Journal of Polymer Science Part a-Polymer Chemistry* **2010,** *48* (2), 454-462.

66. Yamamoto, M.; Uchimura, N.; Adachi, K.; Tsukahara, Y., *Designed Monomers and Polymers* **2010,** *13* (5), 445-458.

67. Wurm, F.; Lopez-Villanueva, F. J.; Frey, H., *Macromolecular Chemistry and Physics* **2008,** *209* (7), 675-684.

68. Xie, C.; Ju, Z. H.; Zhang, C.; Yang, Y. L.; He, J. P., *Macromolecules* **2013,** *46* (4), 1437-1446.

69. Jikei, M.; Suzuki, M.; Itoh, K.; Matsumoto, K.; Saito, Y.; Kawaguchi, S., *Macromolecules* **2012,** *45* (20), 8237-8244.

70. Han, J.; Zhu, D. D.; Gao, C. *Polymer Chemistry* **2013,** *4* (3), 542-549.

71. Jikei, M.; Uchida, D.; Matsumoto, K.; Komuro, R.; Sugimoto, M., *Journal of Polymer Science Part a-Polymer Chemistry* **2014,** *52* (13), 1825-1831.

72. Matsen, M. W. *J. Chem. Phys* **2000,** *113*, 5539-5544.

73. Yang, J. X.; Li, L. W.; Jing, Z. Y.; Ye, X. D.; Wu, C., *Macromolecules* **2014,** *47* (23), 8437-8445.

74. Masukawa, S.; Kikkawa, T.; Fujimori, A.; Oishi, Y.; Shibasaki, Y., *Chemistry Letters* **2015,** *44* (4), 536-538.

75. Ma, H.; Wang, Q.; Sang, W.; Han, L.; Liu, P.; Sheng, H.; Wang, Y.; Li, Y., *Macromolecular Rapid Communications* **2015**, DOI: 10.1002/marc.201500561.

76. Quirk, R. P.; Wang, Y. C. *Polymer International* **1993,** *31* (1), 51-59.

77. Bates, F. S.; Fredrickson, G. H. *Annu. Rev. Phys. Chem.* **1990**, *41*, 525-557

78. Hamley, I. W. *The Physics of Block Copolymers*, Oxford University Press, (**1998**)

79. Matsen, M. W. *Macromolecules* **2012,** *45* (4), 2161-2165.

80. Kimani, S. M.; Hardman, S. J.; Hutchings, L. R.; Clarke, N.; Thompson, R. L., *Soft Matter* **2012,** *8*, 3487-3496.

81. López-Villanueva, F.-J.; Wurm, F.; Kilbinger, A. F. M.; Frey, H. *Macromol. Rapid Commun.* **2007**, *28*, 704-709

82. Dodds, J. M.; Hutchings, L. R. *Macromol. Symp.* **2010**, *291-292*, 26-35

83. Kempe, K.; Krieg, A.; Becer, C. R.; Schubert, U. S. *Chem. Soc. Rev.* **2012**, *41*, 176-191

84. Hamley, I. W.; Castelletto, V., *Prog. Polym. Sci*. **2004**, *29*, 909-948.

**For Table of Contents use only**

# Chain architecture as an orthogonal parameter to influence block copolymer morphology. The synthesis and characterisation of hyperbranched block copolymers - HyperBlocks.

*Lian. R. Hutchings*[1], Serena Agostini, Ian Hamley[2] and Daniel Hermida-Merino[3]*